7. Disposal

Principles: containment*, dilution, multiple barriers*, ALARA

Disposal options: Where? land, ocean, ice, space; Depth? surface, medium, great; When? 10 y, 100 y, 1000 y; Form? spent fuel, glass, synthetic rock; Geometry? boreholes, repository; Container? metal, ceramic

Site requirements: remoteness, release rate, $, reversibility, radiological safety;

Geological D*: age, stability, shielding, GW, slow; options*: repository (1, n-levels), boreholes

Alternative D: space, islands, ocean, technological, storage (N)

Space*: $, risk, Challenger 1986/1, russian satellite 1978;

Ice sheet*: remoteness, self-sinking, $, legal constraint, isolation;

Ocean**: self-burying, sedimentation zones, boreholes, +:R, dilution, RS -: $, LDC

Islands: barriers: rock + ocean, little GW, $; continental I: igneous, metamorphic, sedimentary rocks; oceanic I: basalt; island arcs: plate boundaries, andesitic volcanism;

rock melting*: radiogenic heat 100 kW/m^3, modelling of magma

transmutation: I-129, Tc-99,$, radiation exposure, more LLW+LLW

very deep hole*: T

Release processes: caused by water, waste, man, nature;

man: inadvertent intrusion, drilling, metallic cone, mining, records; waste: radiation damage, radiolysis, thermal (expansion, convection), criticality; nature: slow processes (sea level change, erosion, tectonic movements, magma intrusion, diapirism, glaciation), fast processes (earthquakes, volcanic eruptions, meteorite impact, flooding, hurricanes); groundwater: nominal case + other causes

Normal case*: near-field + far-filed::: GW intrusion, degradation of engineered barriers, RI migration; backfill, swelling, seals, corrosion, radiolysis; container failure, waste dissolution, colloids; transport path, sorption, precipitation

NFE factors : T, stress field, hydrogeology, chemistry::::

T: heat output*, depth 1 km t = 25-50 C, T profile of NF*, heat transfer calc., T max 100 C (US 250 C), corrosion; hydrostatic, lithostathic S, 1 km : 1000 atm, interconnection of fissures, anisotropy, horizontal = 4X vertical + swelling S max 12000 atm + heat stress - spalling, fracturing, stress readjustment; local, regional, hydraulic conductivity; pH, Eh, ionic force, solubilities, thermodynamic calc., computer codes, speciation, colloids, microorganisms, complexants;

Performance of EB: buffer, backfill, container, waste matrix::::: ?: water access + chemistry, ion exchange, properties (thermal conductivity, plasticity, porosity, permeability, swelling pressure, redox potential, sorption, Kd), reactions (MM + K - illite), bentonite clay (Na montmorillonite) + quartz, P = 1E-13 m/s, buffers pH>7, FeSiO4; ? IE,. cement grout, powdered basalt, air; ?:

protection 500 -10 000 y, handling, shielding, types (M, ceramic, M+C), materials (Cu, Ti, SS, Fe), sealing techniques, corrosion (complexes, electrochemical techniques, pitting, SCC, Radiation, H2, O2); glass, spent fuel:: leach testing (static, dynamic, Soxhlet, T, realistic); kinetics*, slow at 25 C, fast at 200 C;

Composition of high-level borosilicate waste glass. Container weight = 480 kg; glass weight = 405 kg/container. Added oxides (%) : SiO_2 45, B_2O_3 14, Al_2O_3 5, Na_2O 10, CaO 4, Fe_2O_3 3, NiO 0.4, Cr_2O_3 0.5, P_2O_5 0.3, ZrO_2 1, Li_2O 2, ZnO 2.5.; Fission product oxides : 11.1%, Actinide oxides : 0.9%, Metallic particles 0.7% Actinides g/container: Am 423, Cm 33, Pu 80, Np 573, U 1920.

Spent fuel: UO2, FP diluted, redox, carbonates, 25 C + 8 y: MD = 1E-6/d to 1E-9/d, grain boundaries: Cs,I, Sr, colloids

Modelling NF: granite, 1.2 km, Fe 25 cm thick, GW: 4200 l/y, T max 160 C, Material inventory (per waste container) in the near-field of a reference Swiss high-level waste repository*

Material	Volume (m^3)	Mass (kg)
Glass	0.15	405
Steel-fabrication container	0.01	75
Fabrication void	0.03	-
Canister	0.9	6500
(a) Bentonite (dry)	32.7	88000
(b) Pore space (water-filled)	20.1	20000

corrosion 1300 y, ph 7-8.5, 1E-7 $g/cm^2/d$ 1E-5 of inventory/y, dissolution in 0.7 l/canister/y

Fission activation product inventory 1000 years after disposal in the Swiss reference HLW repository.

Release rate limited by: dissolution solubility

RI	T - y	I -mol	Mol/y	Bq/y	Mol/y	Bq/y
10-Be	1.6E+6	2.6E-5	5.1E-10	4.2E+0	7.1E-5	5.9E+5
14-C	5.7E+3	1.9E-5	3.7E-10	8.5E+2	high	high
41-Ca	1.3E+5	8.7E-5	1.7E-9	1.7E+2	7.1E-3	7.2E+8
59-Ni	8.0E+4	1.1E-2	2.2E-7	3.6E+4	7.1E-5	1.2E+7
79-Se	6.5E+4	9.3E-2	1.8E-6	3.7E+5	7.1E-9	1.4E+3
90-Sr	29	6.1E-10	1.2E-14	5.5E+0	7.1E-5	3.2E+10
93-Zr	1.5E+6	1.1E+1	2.2E-4	1.9E+6	7.1E-10	6.3E+0
94-Nb	2.0E+4	3.9E-4	7.6E-9	5.0E+3	7.1E-9	4.7E+3
99-Tc	2.1E+5	1.1E+1	2.2E-4	1.4E+7	2.3E-8	1.4E+3
107-Pd	6.5E+6	2.5	4.9E-5	1.0E+5	7.1E-9	1.4E+1
126-Sn	1.0E+5	3.6E-1	7.0E-6	9.3E+5	7.1E-10	9.4E+1
129-I	1.6E+7	1.8E-3	3.5E-8	2.9E+1	high	high
135-Cs	2.3E+6	3.2	6.2E-5	3.6E+5	high	high
137-Cs	30	2.0E-8	3.9E-13	1.7E+2	high	high
147-Sm	1E+11	1.5	2.9E-5	3.5	7.1E-9	8.5E-4

I = Inventory

P = porosity (0.38), D = density (2760 kg/m^3)
retardation : R = 1 + (1-P)*D*Kd/P = 1 + 4500 Kd; 24< R <23000, conc. > 10 Bq/l Cs-135, Se-79, Pd-107, Tc-99, Sn-126.

Limitations: simplification, radiolytic oxidants, colloids,

microorganisms
Far-field: massive physical + chemical buffer, path length, migration velocity; salt*, clay*, granite*
RI migration: advection, diffusion; water table(m - Dm), NTS Hm, hydraulic pressure or head* {m} (topography, conductivity (fractures)), Darcy law : Q=K*I*A; porous media, channelling, effective porosity (clay P = 30%, EP = 5%), variability
Maximum and minimum values for the hydraulic conductivity (HC), porosity (P), gradient (G), flux (F) and velocity (V) of various sediments and crystalline rocks, in typical environments which might be considered for disposal purposes.

Rock type	Depth - m	HC - nm/s	P	G	F - l/y/m²	V - m/y
Clay	0-100	0.1,	0.3,0.5	0.05,0.2	1.6,640	0.0005,1.28
Clay	<100	1E-3,10	0.3,0.5	0.05,0.2	0.002,64	5E-6,0.1
Shale	0-100	1,1000	0.2,0.3	0.05,0.2	1.6,6400	0.008,21
Shale	<100	0.1,100	0.05,0.25	0.05,0.2	0.16,640	0.003,2.6
Crystalline	0-100	1,100	0.01,0.05	0.001,0.1	0.03,320	0.003,6.4
Crystalline	<100	0.01,10	0.001,0.01	0.001,0.1	0.0003,32	0.0003,3.2
Aquifer		10,1E+5	0.05,0.1	0.0005,0.01	1.6,32000	0.03,320

Transport models: HC, depth, near surface flow lines* ~100 y, deep lines 1E+4 - 1E+6 y, islands - sea, Herzberg lens flow ~0; physical dispersion*: dispersion coef., late arrivals, tortuosity, 2D case - 3 parameters, 3 D - 6 p, isotropy, percolation theory; diffusive retardation: rock P = 2% EP = 0.1% dead end pores*; chemical retardation*: precipitation, sorption (cations), Kd, Pu, Tc, Np, Migration in evaporites: impermeable, diapirism, flooding, faults

The distribution of radionuclide ingestion doses over various pathways for the Swiss Project 1985. The values are given as a percentage of the total dose from each radionuclide, and apply to the biosphere transport reference case used in the assessment.

RI	DW	Milk	Meat	Wheat	RV
U-238	96	1	1	2	1
Ni-59	86	3	2	5	3
Se-79	30	3	66	1	1
Tc-99	21	54	1	15	8
Pd-107	86	3	2	5	3
Sn-126*	12	5	1	63	17
Cs-135	37	22	23	8	7

DW = Drinking water, RV = Root vegetables, * Short-lived daughters taken into account, l= less than 0.5%.

Summary of element retention in the Oklo fossil reactor zones: Elements which mostly migrated: Kr, Sr, Mo, Ag, Cd, I, X, Cs; Elements which were mostly retained : Y, Zr, Nb, Rh, Pd, In, Sn, Sb, light REE, Po, Th, U, Np, Pu; Elements which were locally redistributed : Rb,Tc, Ru, heavy REE

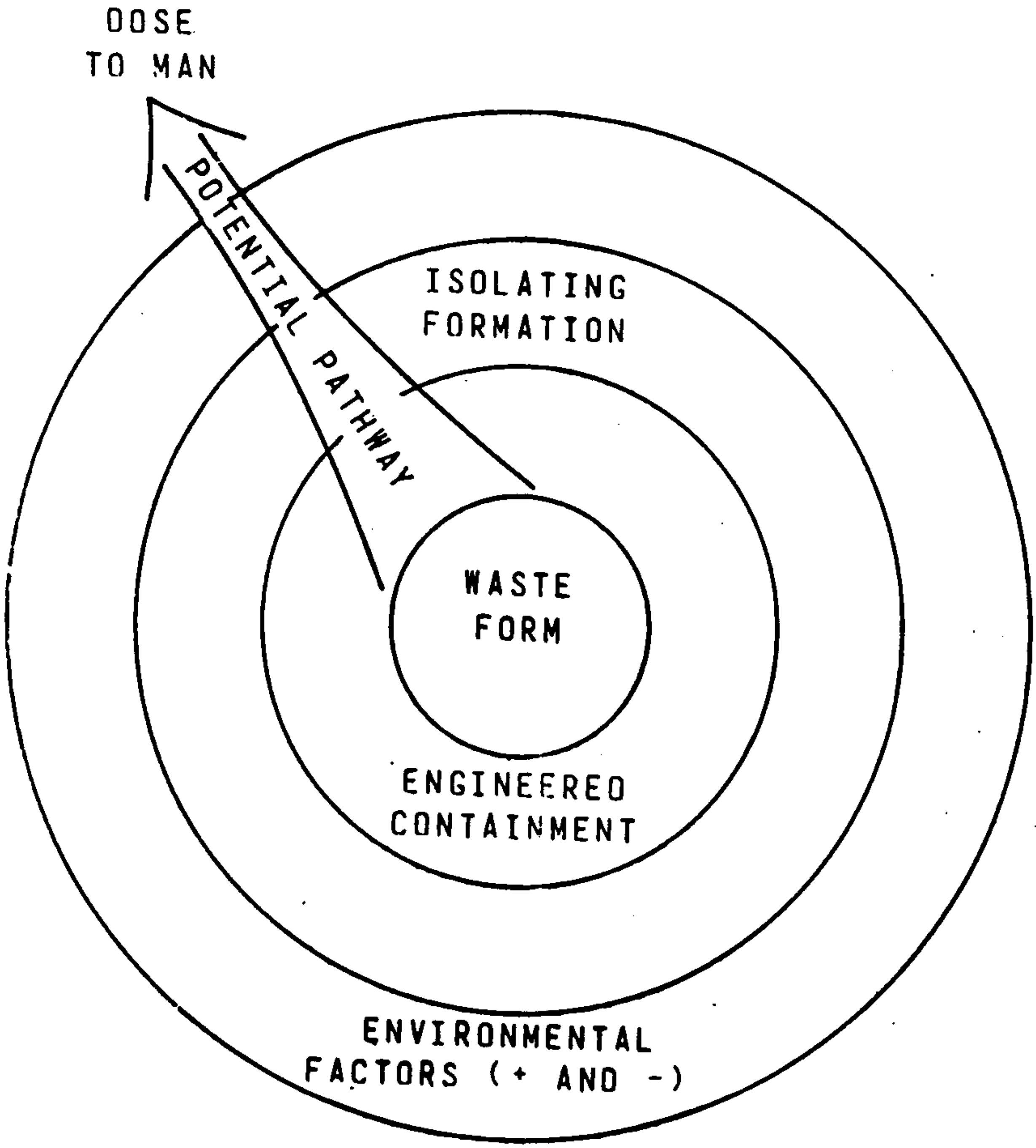

FIGURE 1 MULTIPLE-BARRIER CONCEPT OF WASTE DISPOSAL

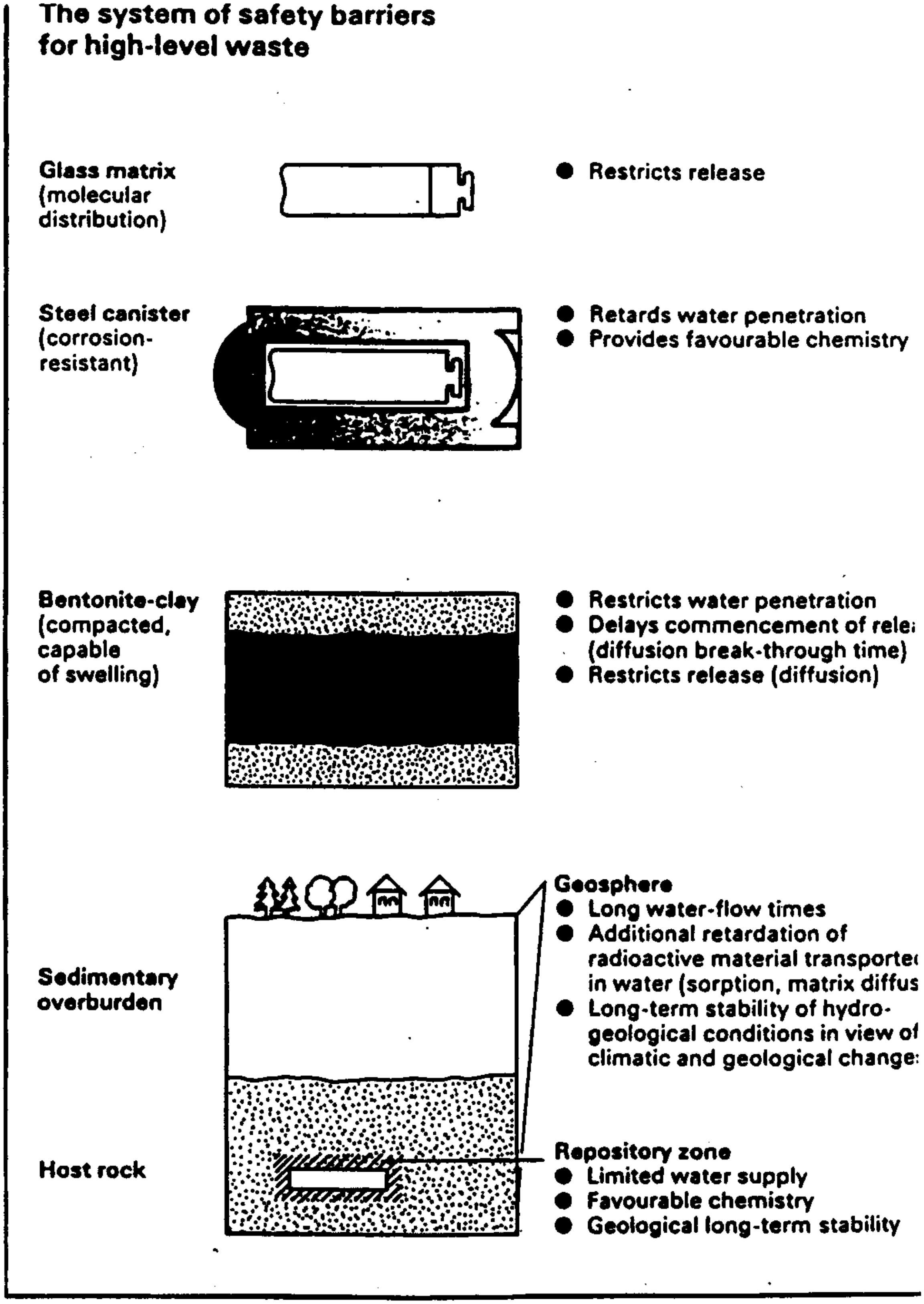

Figure 4.2 Schematic illustration of the multi-barrier system of waste containment; instance the Swiss concept for disposal of high-level waste. *Reproduced by permis. Nagra, Switzerland* Chapman 87

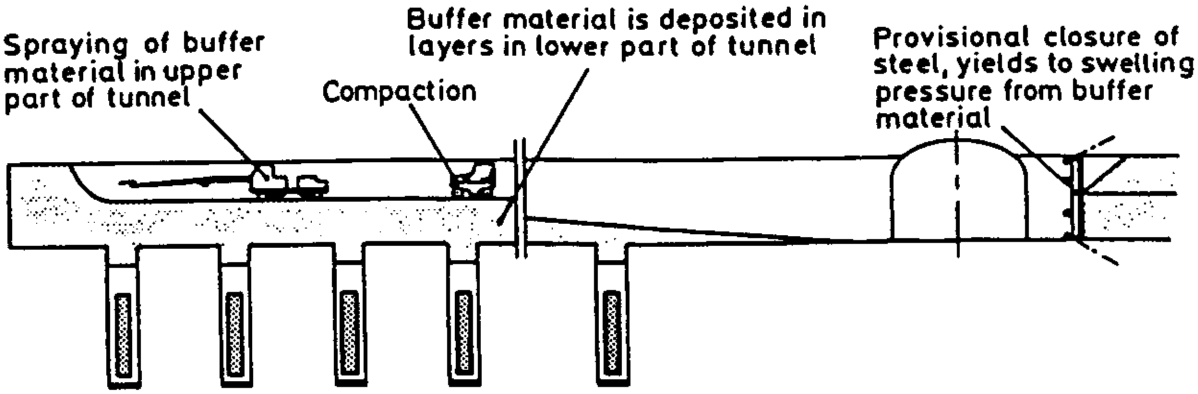

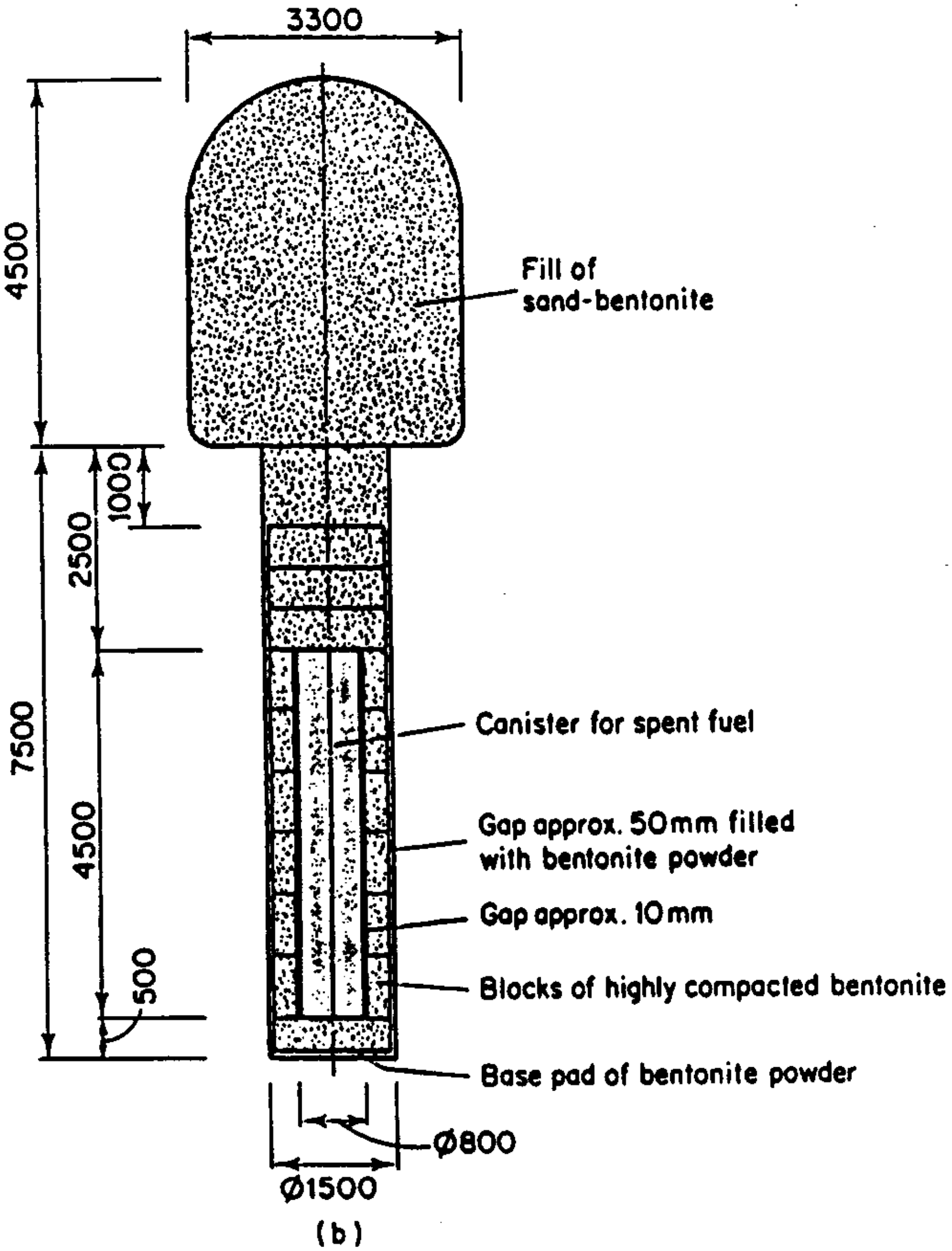

Figure 4.3 Alternative emplacement techniques for high-level waste containers in a deep repository in hard rock. (a) The Swiss concept for in-tunnel disposal. (b) The Swedish concept for disposal in shallow boreholes below the tunnel floor. Both concepts use a buffer material of highly-compacted bentonite around the waste containers, emplaced as preformed blocks (dimensions in mm). *Reproduced by permission of Nagra, Switzerland and SKB, Sweden*

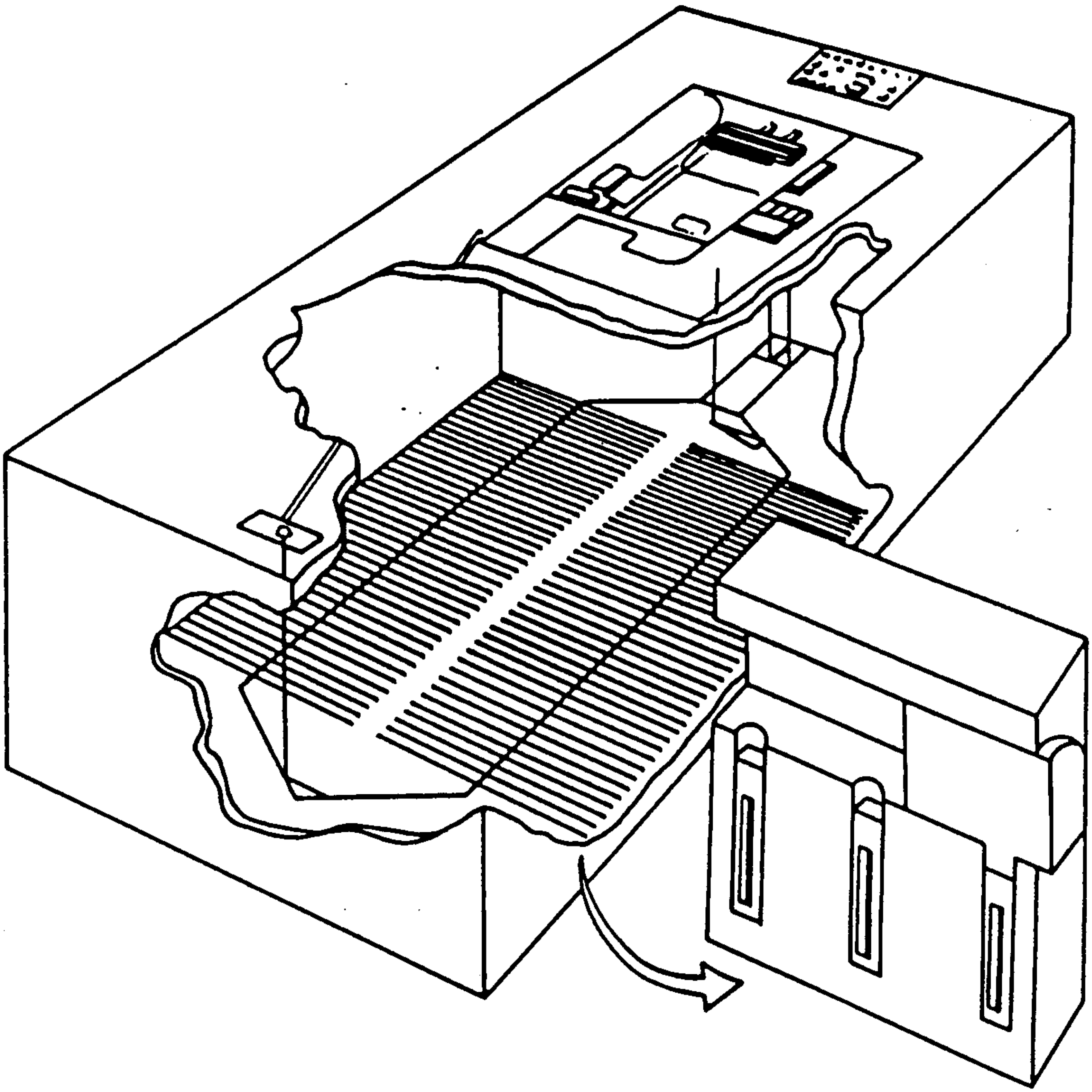

Figure 4.4 Cutaway diagram of the Swedish concept for a high-level waste repository at a depth of about 500 m in hard crystalline basement rocks, using the container emplacemen technique shown in Figure 4.3(b) (courtesy of SKB)

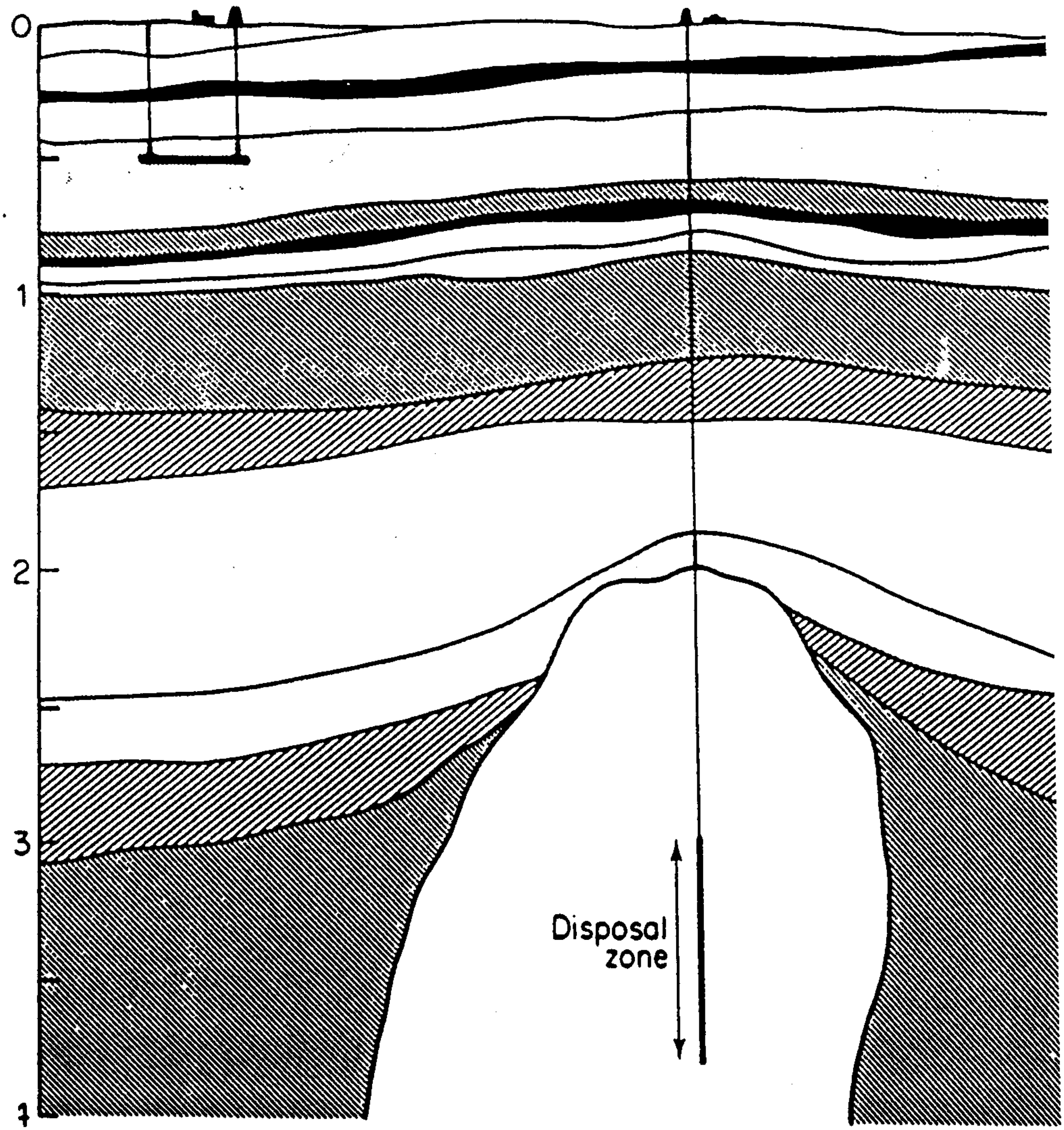

Figure 4.1 Schematic illustration of the deep repository concept for long-lived waste disposal (in this case at a depth of some 500 m in a clay formation) compared to the deep borehole disposal concept (in this case at depths greater than 2000 m in a salt dome)

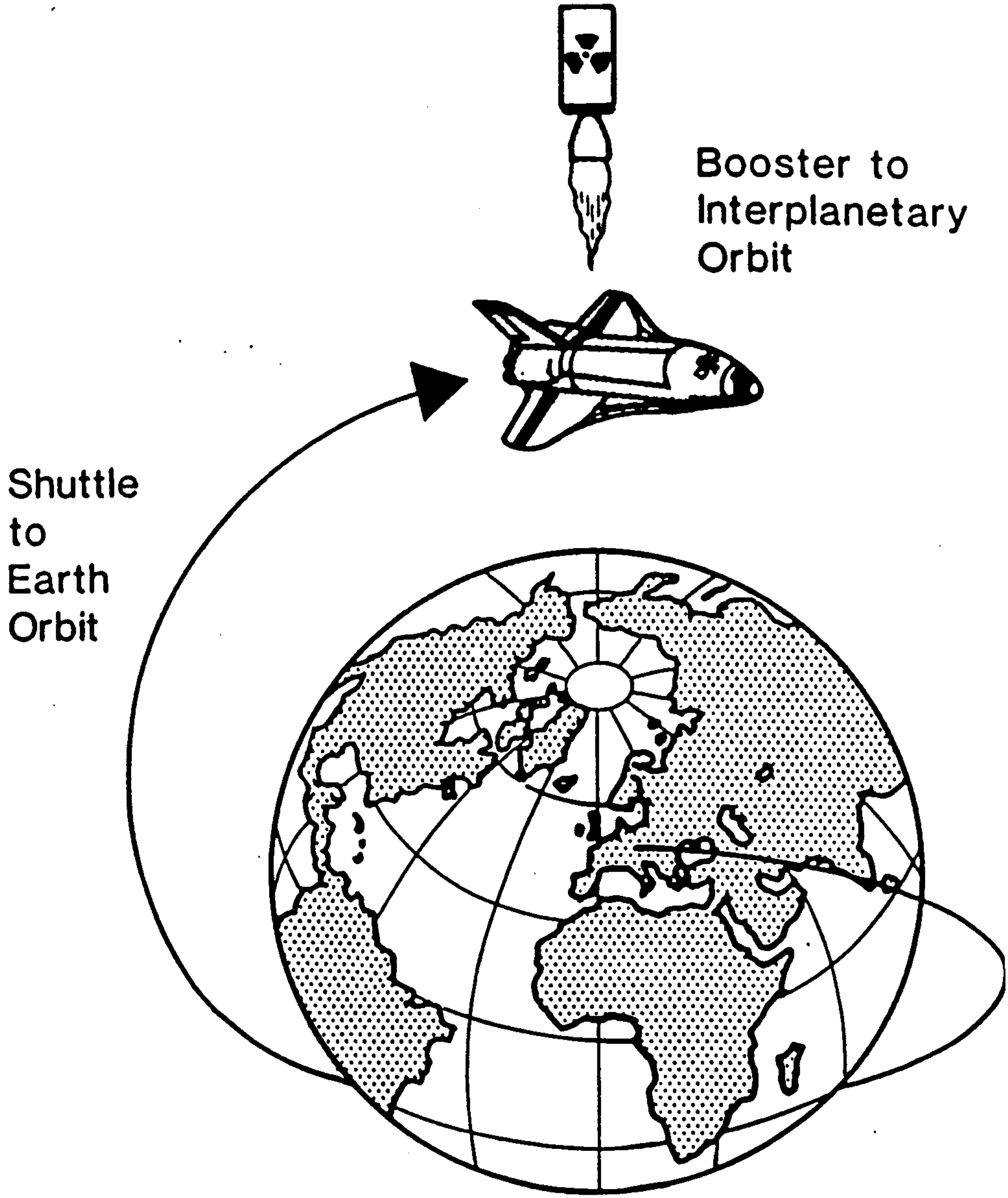

Figure 3.2 Conceptual space disposal system for high-level wast(
which would use the space shuttle and allied technology to depos

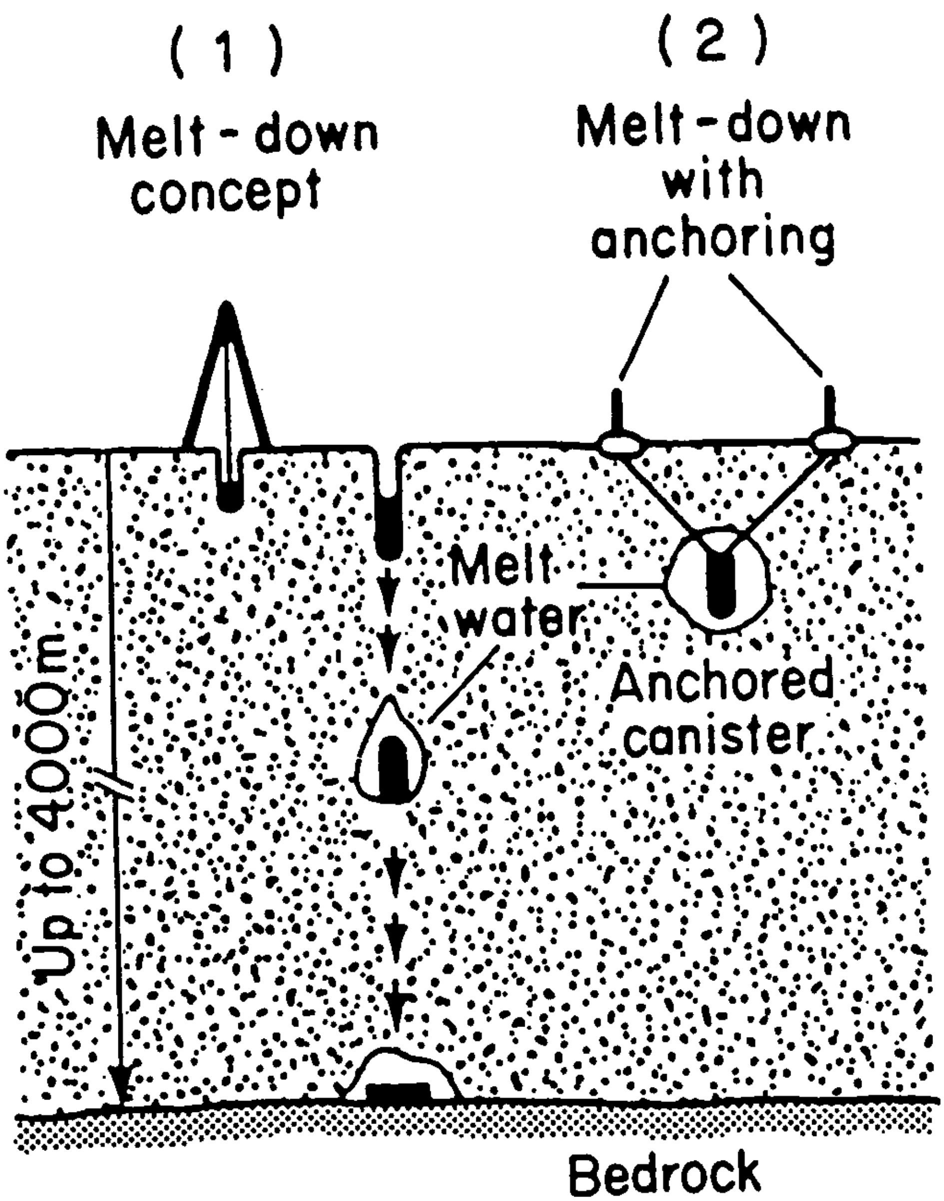

Figure 3.3 Old, and now largely discredited, concepts for disposal of high-level waste below an icecap such as Antarctica or Greenland. (1) Melting concept whereby the wastes own heat eventually brings containers to the base of the ice by melting and (2) a similar concept which prevents the containers from sinking to the bedrock

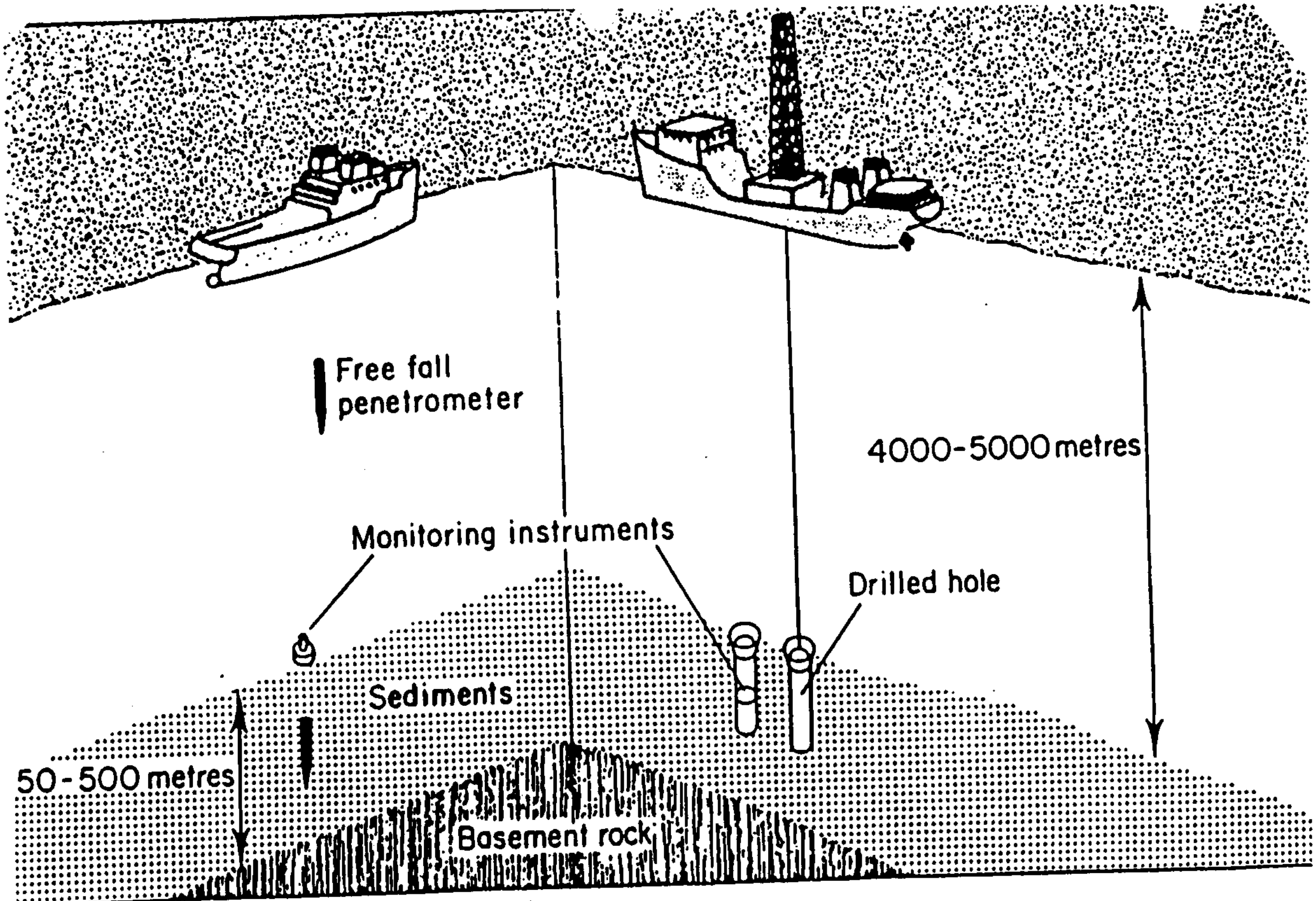

'igure 3.4 Sub-seabed disposal options for high-level waste in the deep ocean basin
'ontainers of waste free-fall from a ship in a streamlined outer penetrator package an
ome to rest some tens of metres below the seabed in the stable soft sediment
lternatively waste packages are emplaced in purpose drilled boreh... in th

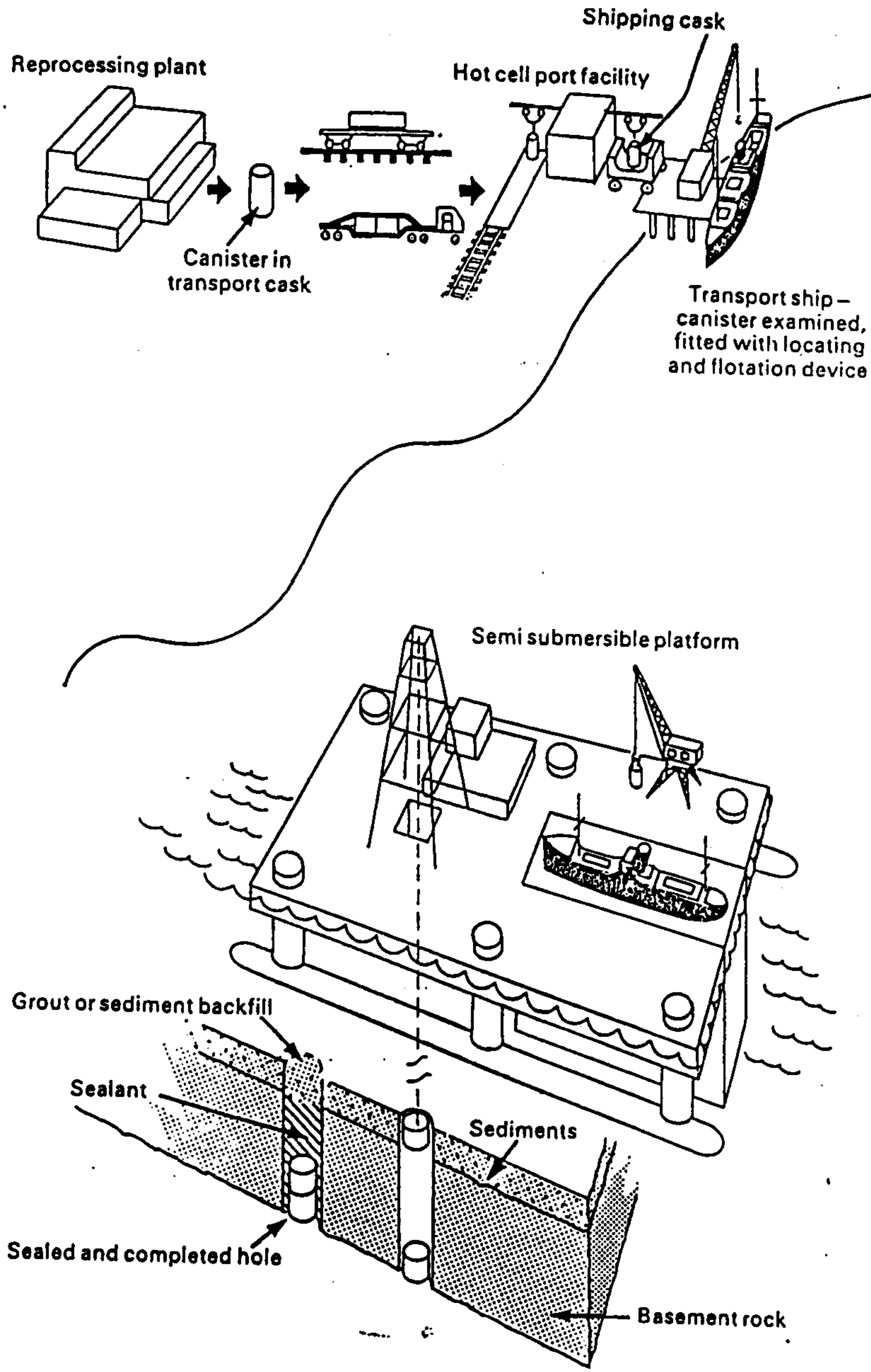

F1

Diagram showing the major components of a system for disposing of radioactive waste in the ocean bed.

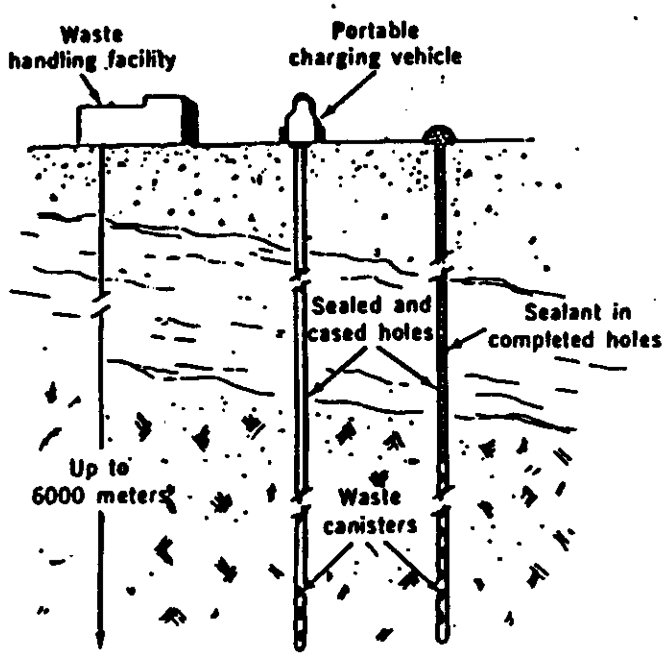

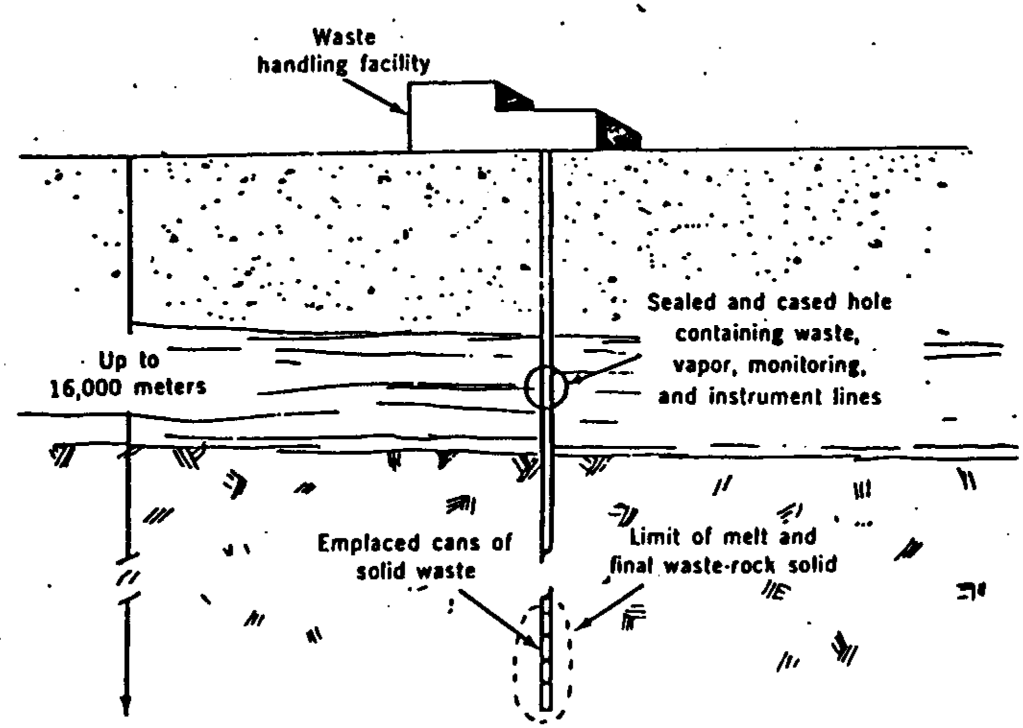

Fig. 4 (left). Solid waste emplacement in a matrix of drilled holes with no melting. [From Schneider and Platt (9)] Fig. 5 (right). Solid wa: emplacement in a deep hole with in-place conversion to a rock waste matrix. [From Schneider and Platt (9)]

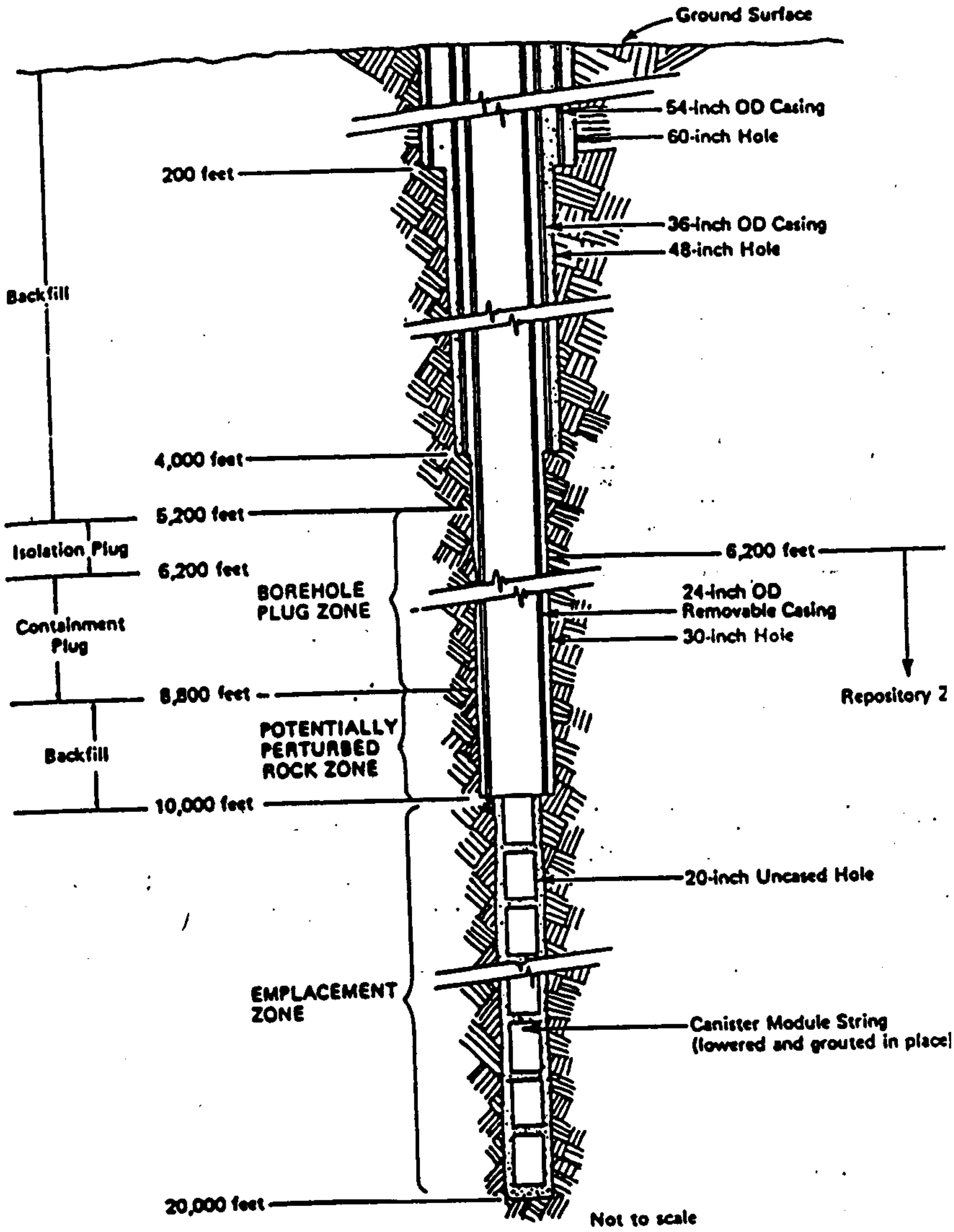

Fig.6.11. Very deep borehole concept for emplacement of high-level waste developed by ONWI /6-31/

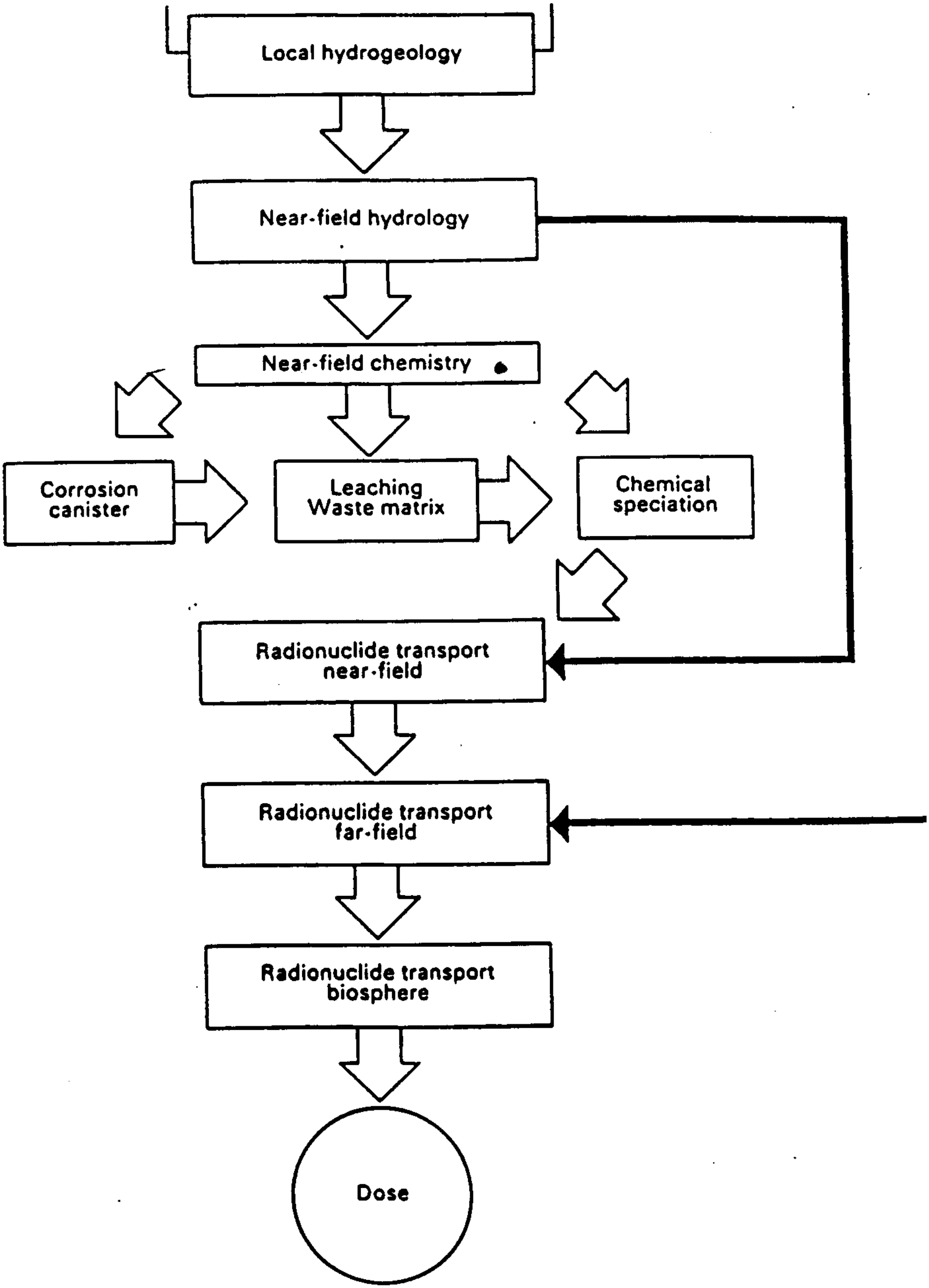

Figure 4.9 A typical normal-case model chain for safety analysis purposes (f
Nagra, 1985). *Reproduced by permission of Nagra, Switzerland*

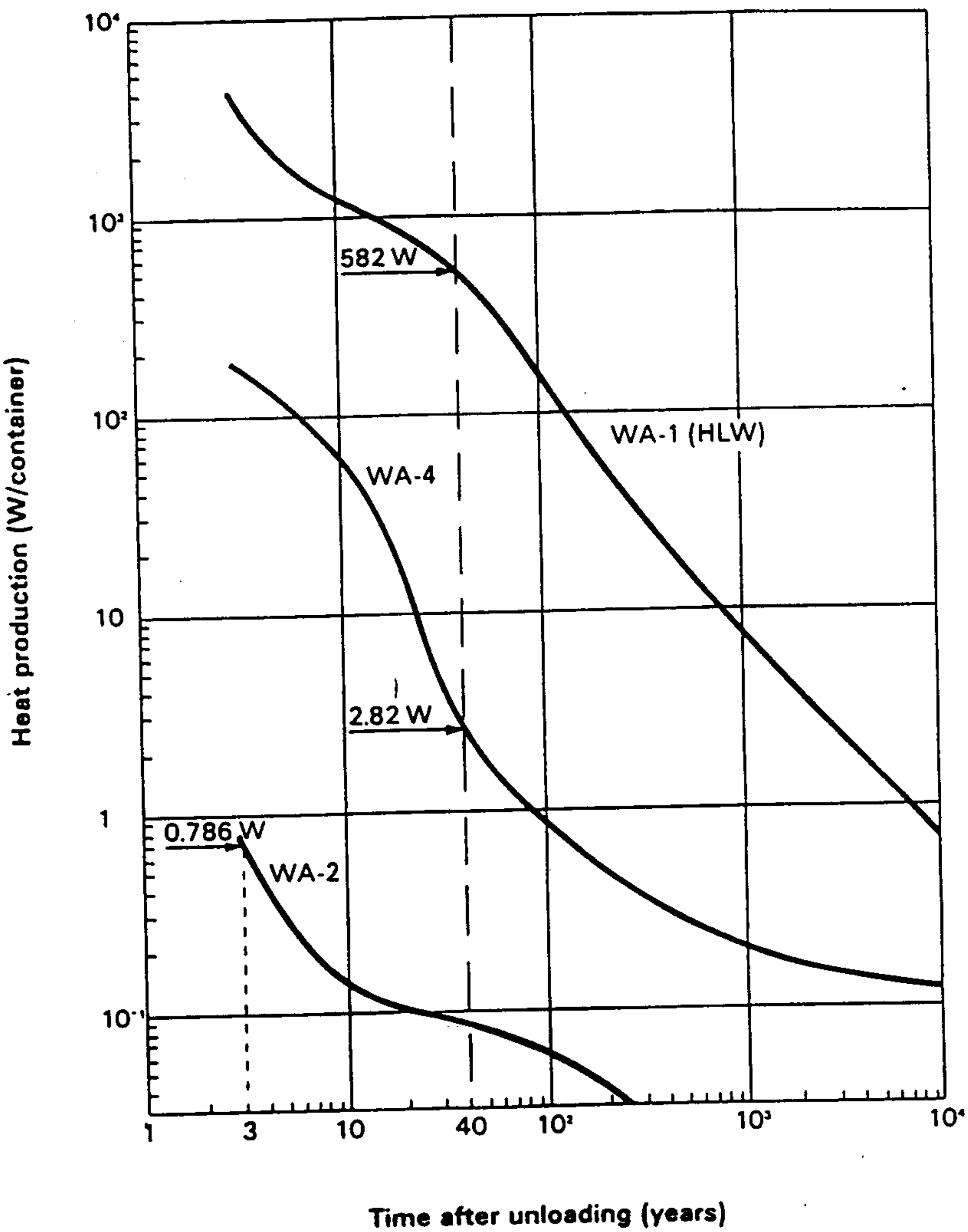

Figure 4.5 The decrease in radioactive decay heat output of different waste types as a function of time, using Swiss waste types as an example. WA–1 is vitrified high-level waste, with an initial heat output of several kilowatts per container; WA–4 is a higher activity intermediate level waste (largely fuel element cladding debris from reprocessing), with an initial heat output of some hundreds of watts per container, and WA–2 is a lower activity ILW (precipitates and concentrates) with very low thermal output. The

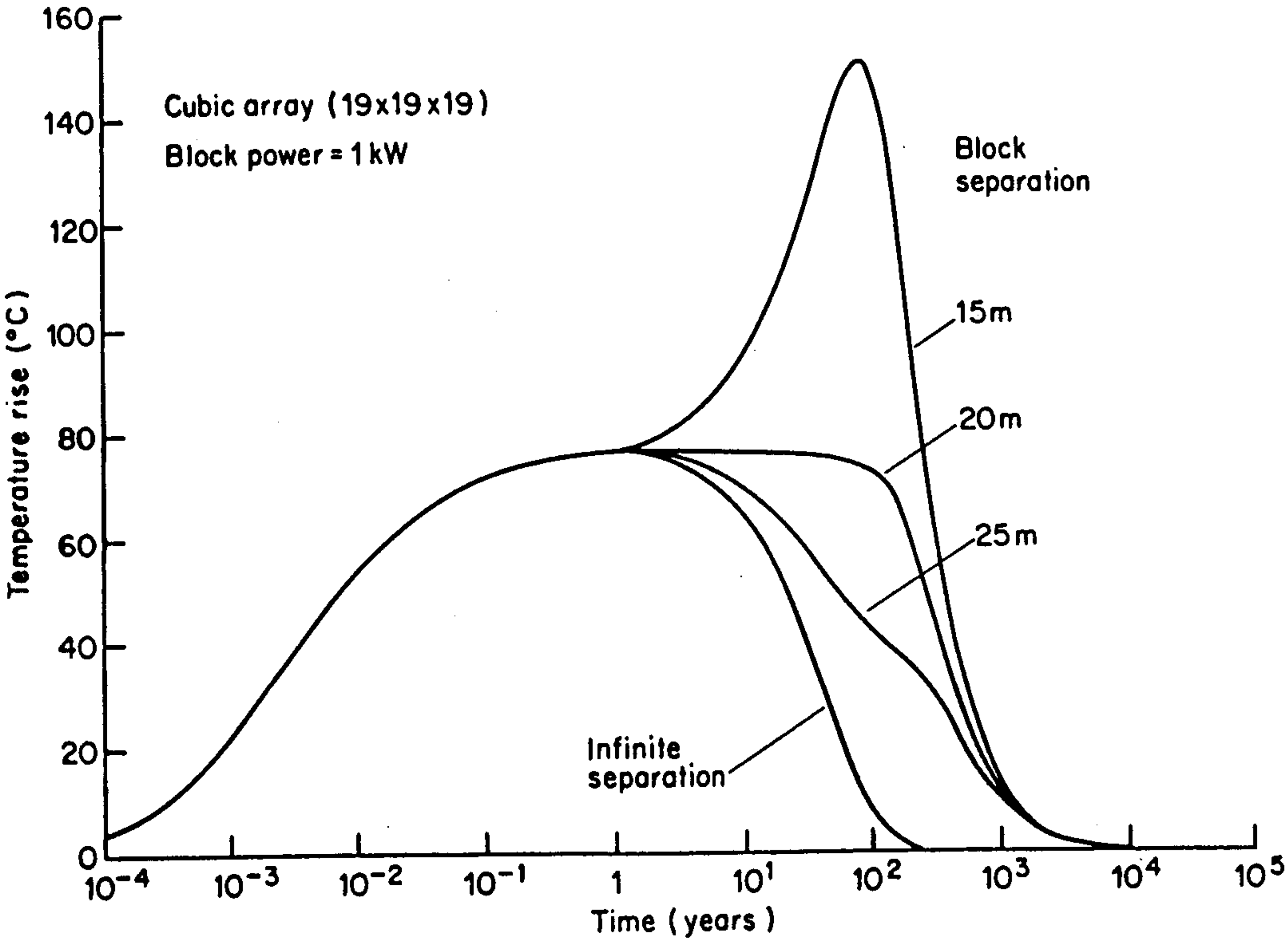

Figure 4.6 The effect of various container separation distances on the maximum temperature rise in the host-rock in a granite HLW repository. If the containers are less than 15 m apart then a sharp rise in temperature occurs after about 100 years. Conversely it can be seen that placing the containers any more than 20 m apart does not give any advantage in terms of maximum repository temperatures. (For a cubic array of 19 × 19 × 19 containers of 1 kW initial heat output at time of disposal: after Hodgkinson.

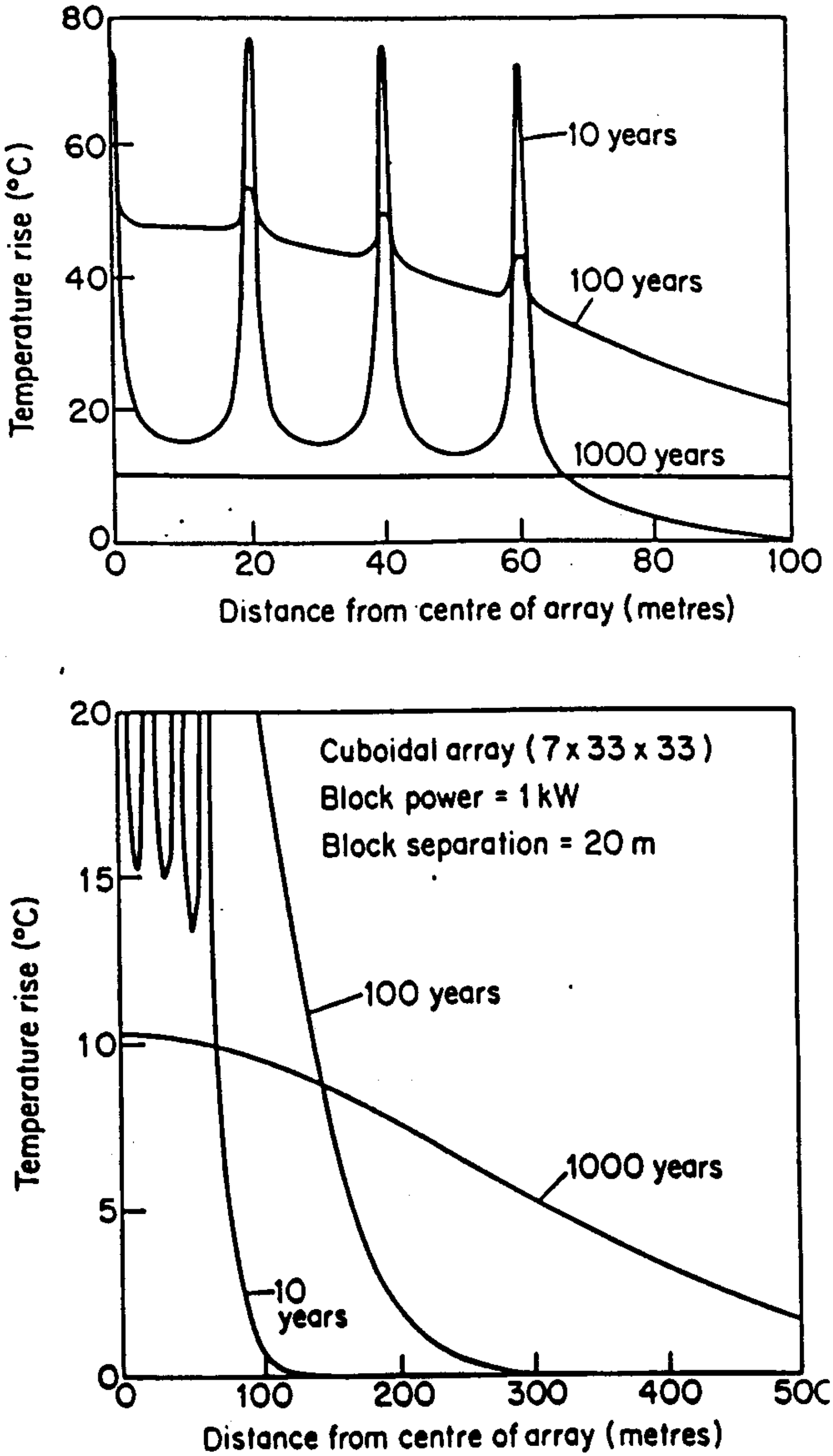

Figure 5.2 Temperature profiles through a complete repository in granite at different times after waste disposal (after Bourke and Hodgkinson, 1977). The calculations are based on a cuboidal array of waste containers of 7 × 33 × 33, with each block of waste having a 1 kW heat

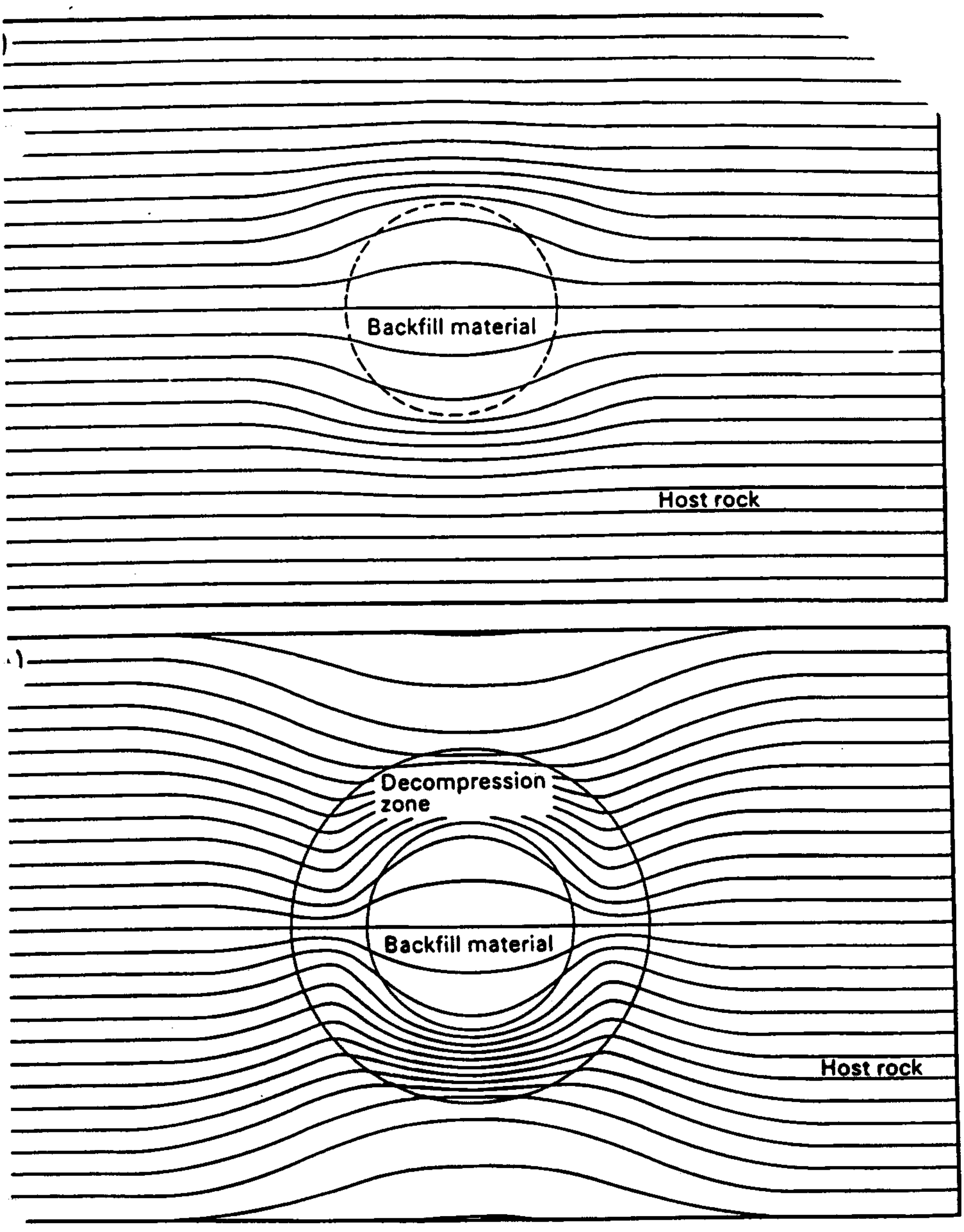

-igure 5.3(a) Theoretical groundwater flow lines, in an homogeneous isotropic dium, around a repository tunnel containing a low hydraulic conductivity backfill. (b)

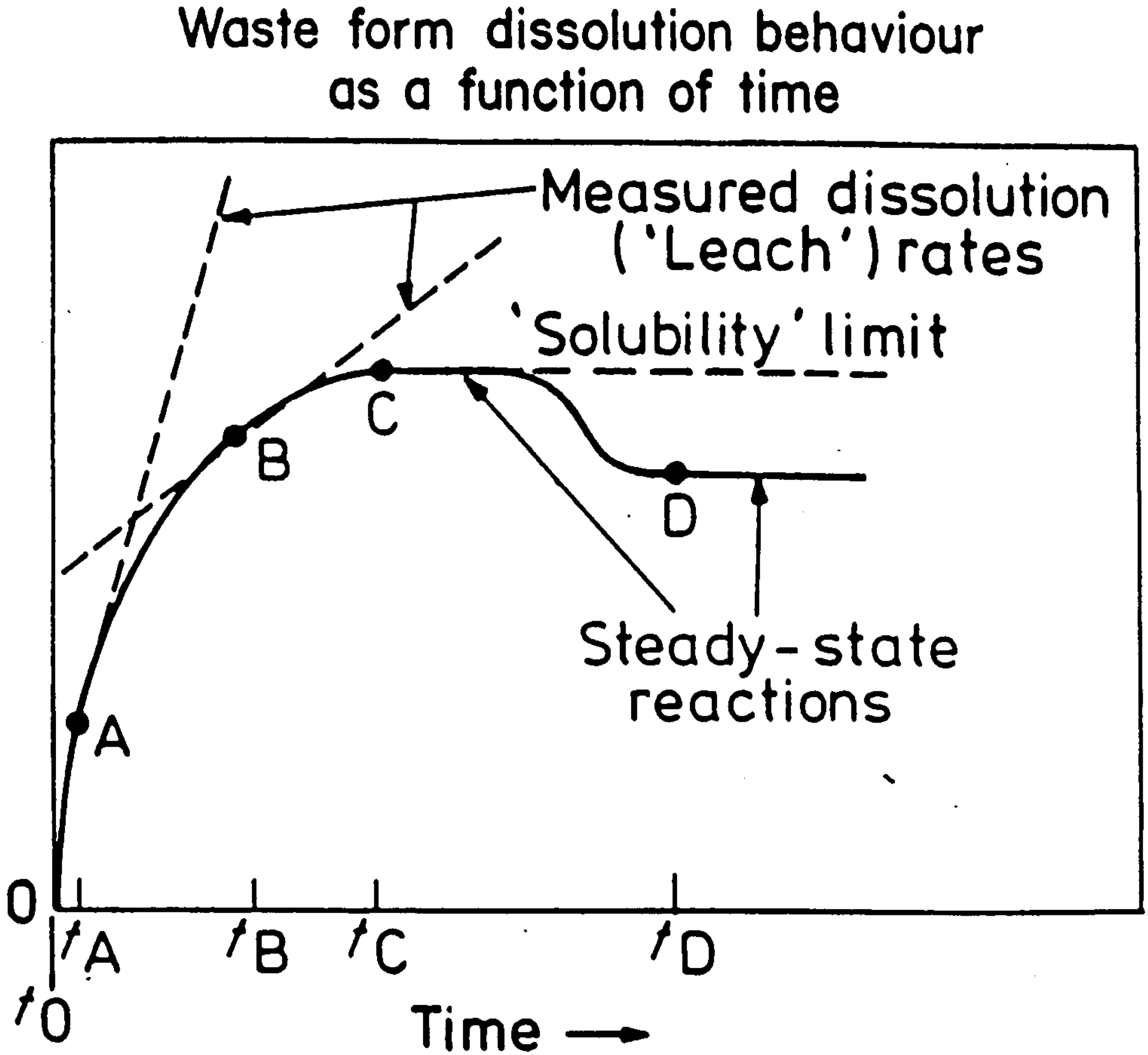

gure 5.4 Theoretical model of waste-forn
ssolution as a function of time in a low-flov
vironment, expressed as the concentration of a
rticular radionuclide in solution in the
oundwater as a function of time; after Savage

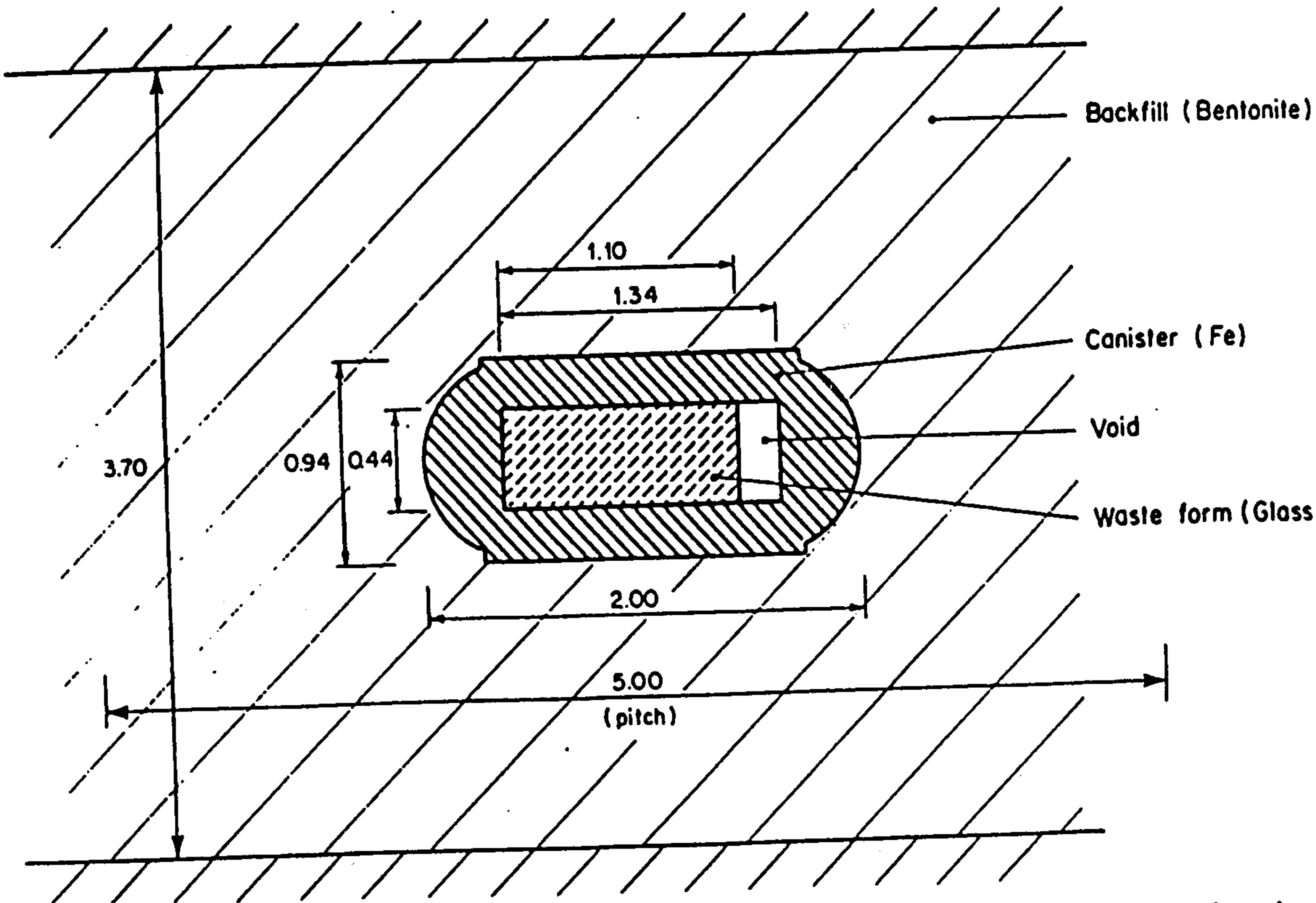

Figure 5.6 Geometry of HLW container emplacement (dimensions in metres) for the Swiss in-tunnel deep repository concept (after Nagra, 1985). *Reproduced by permission of*

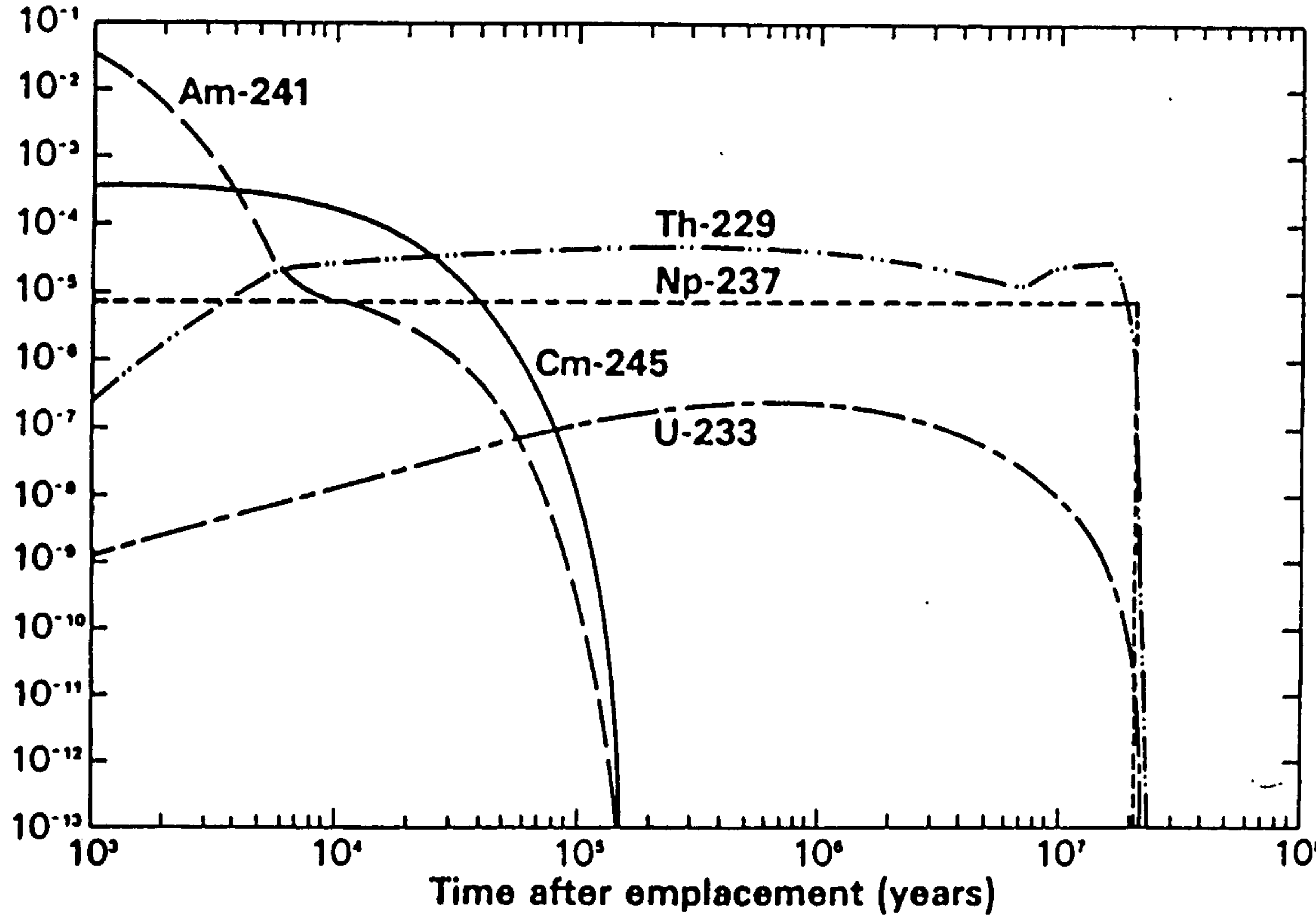

:ure 5.7 Direct release of radionuclides from the waste matrix into the far-field as :
.ction of time after waste emplacement in the repository for the reference case water flu:
1200 l/year through the entire repository (after Nagra, 1985; see text for explanation)

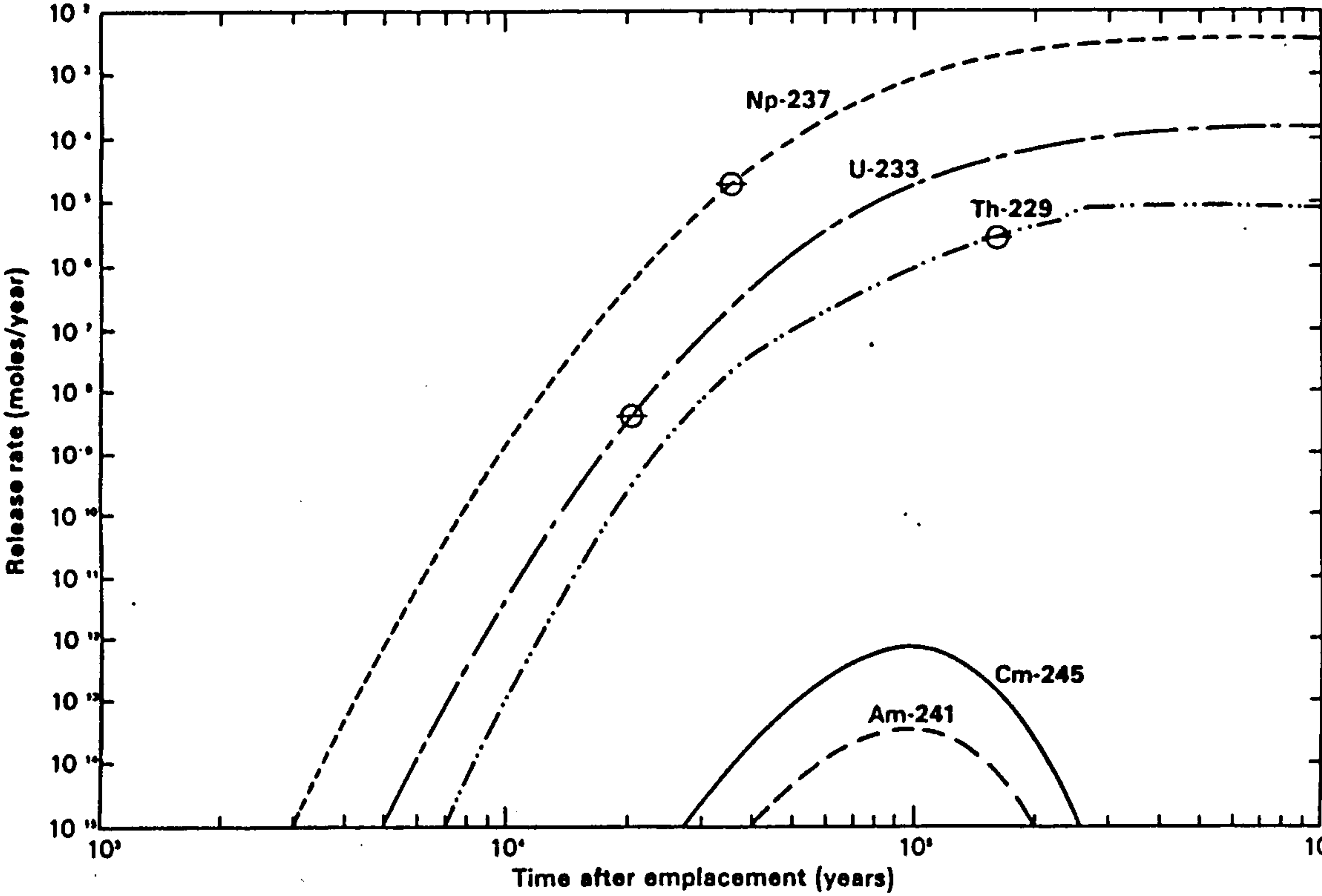

Figure 5.9 Diffusion controlled actinide release rates into the far-field as a function of time after disposal, for the whole repository (Swiss HLW concept), from Nagra, 1985. The points indicate where maximum removal is limited by the solubility of the radionuclide in

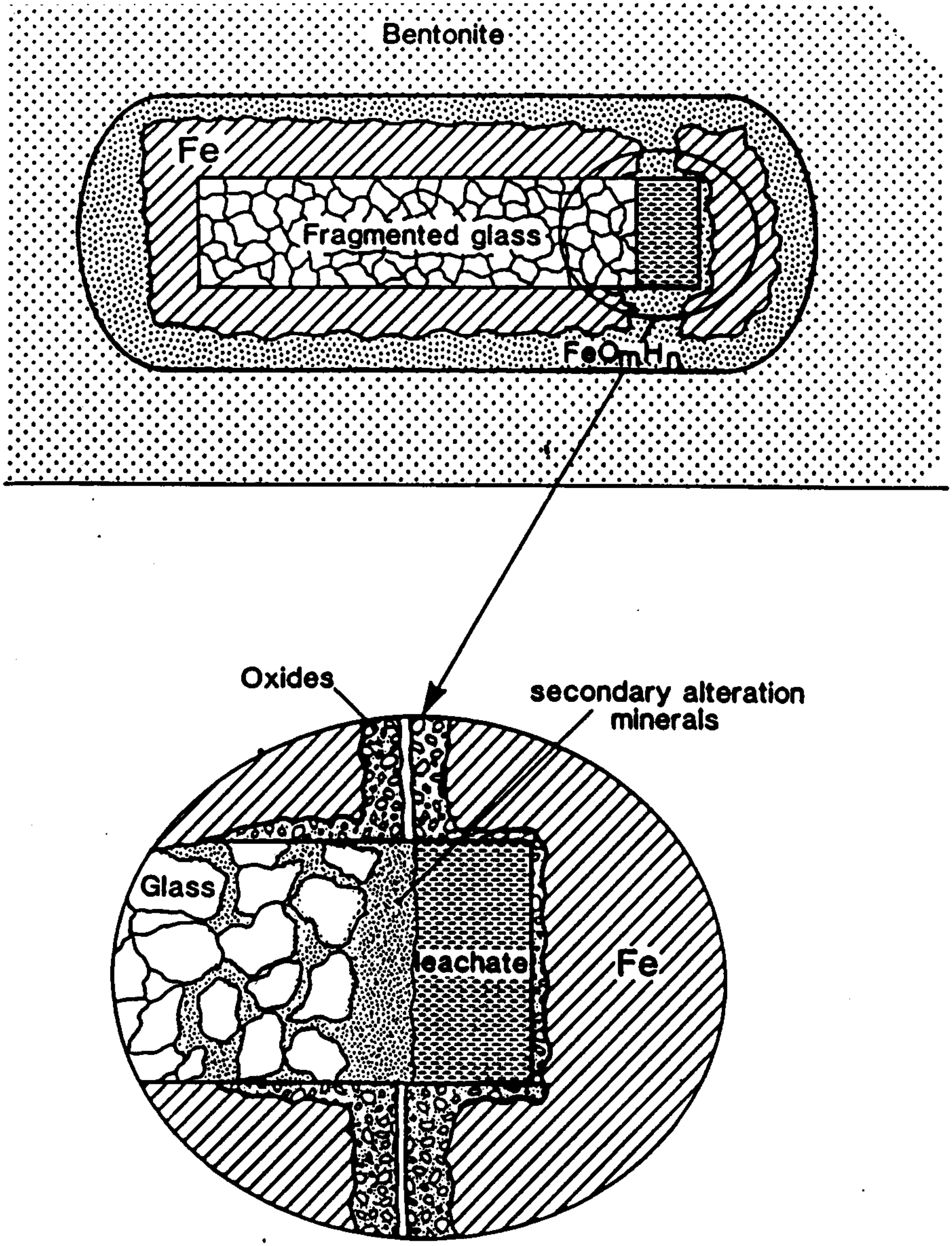

Figure 5.10 Schematic diagram of the near-field in the Swiss HLW repository, after canister failure has occurred, assuming realistic evolution as opposed to the conservative models discussed in the text (after McKinley, 1985a). *Reproduced by permission of Nagra, Switzerland*

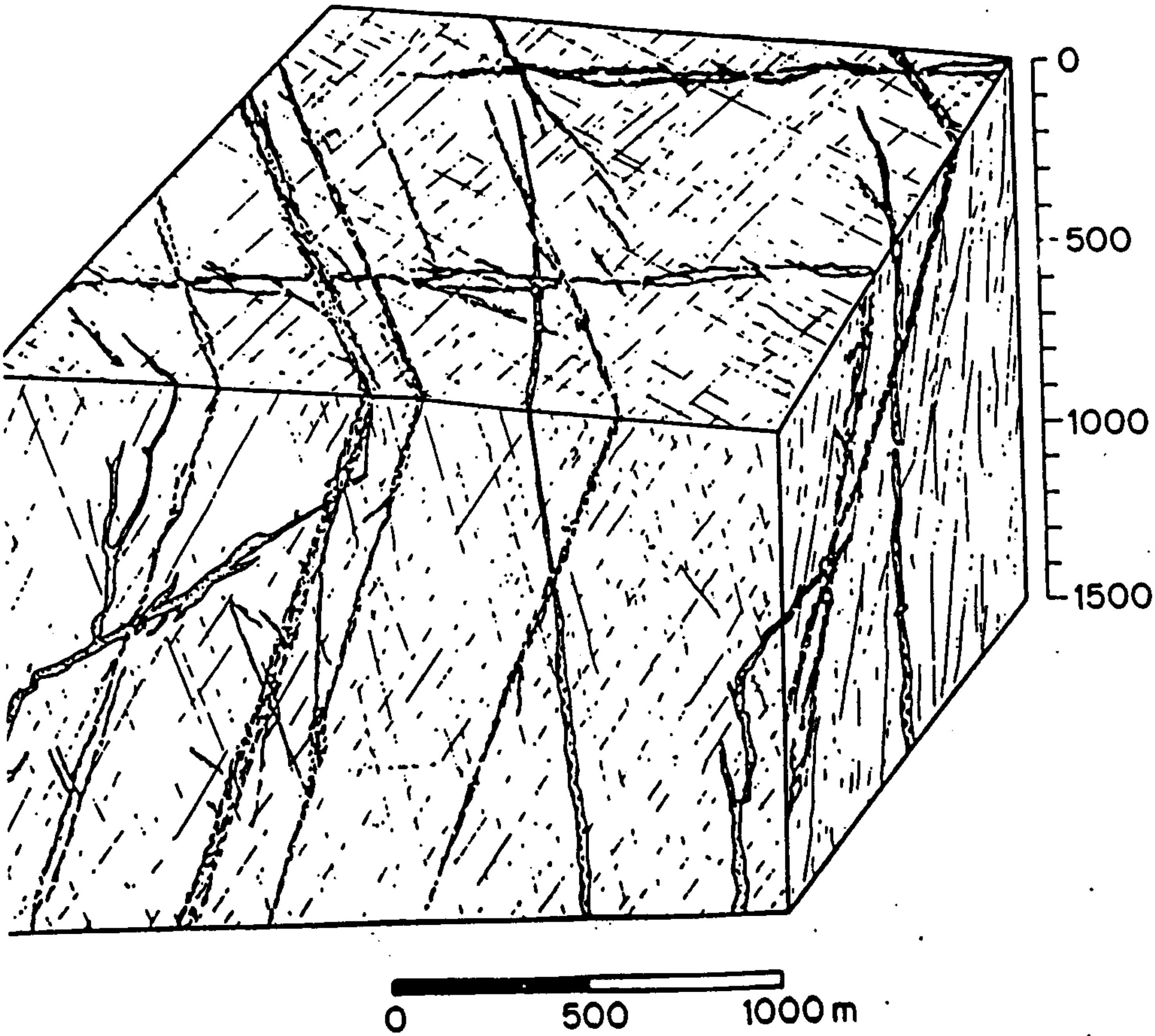

igure 6.1 Schematic illustration of typical joint and fracture patterns in a b
hard crystalline rocks. Irregular major fractures control the bulk of w
ovement in the rock (from Nagra, 1985). *Reproduced by permission of Na*
witzerland

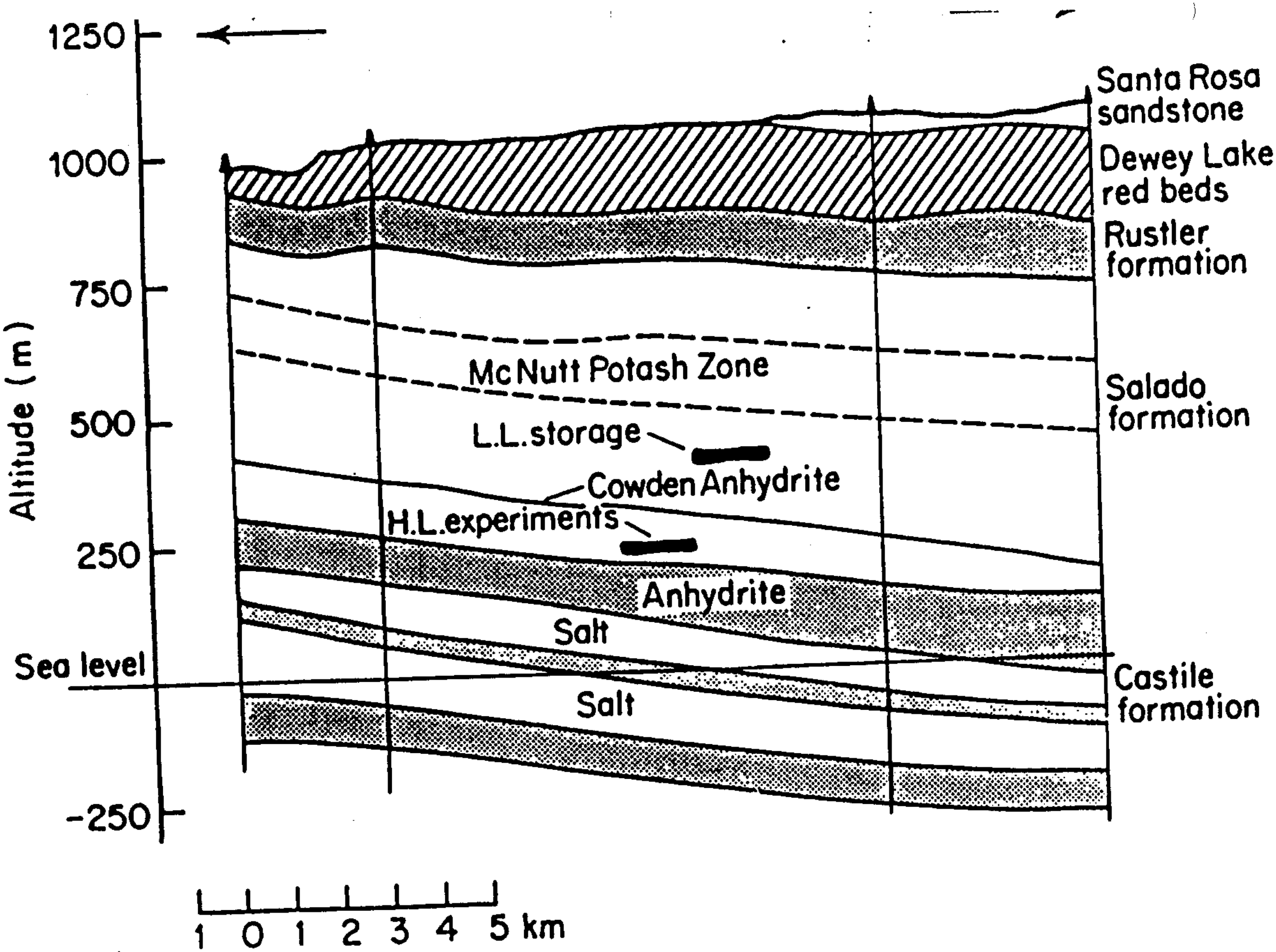

Figure 6.6 Schematic cross-section of the WIPP site in New Mexico, USA, for disposal of long-lived defence wastes in a bedded salt formation (Salado formation)

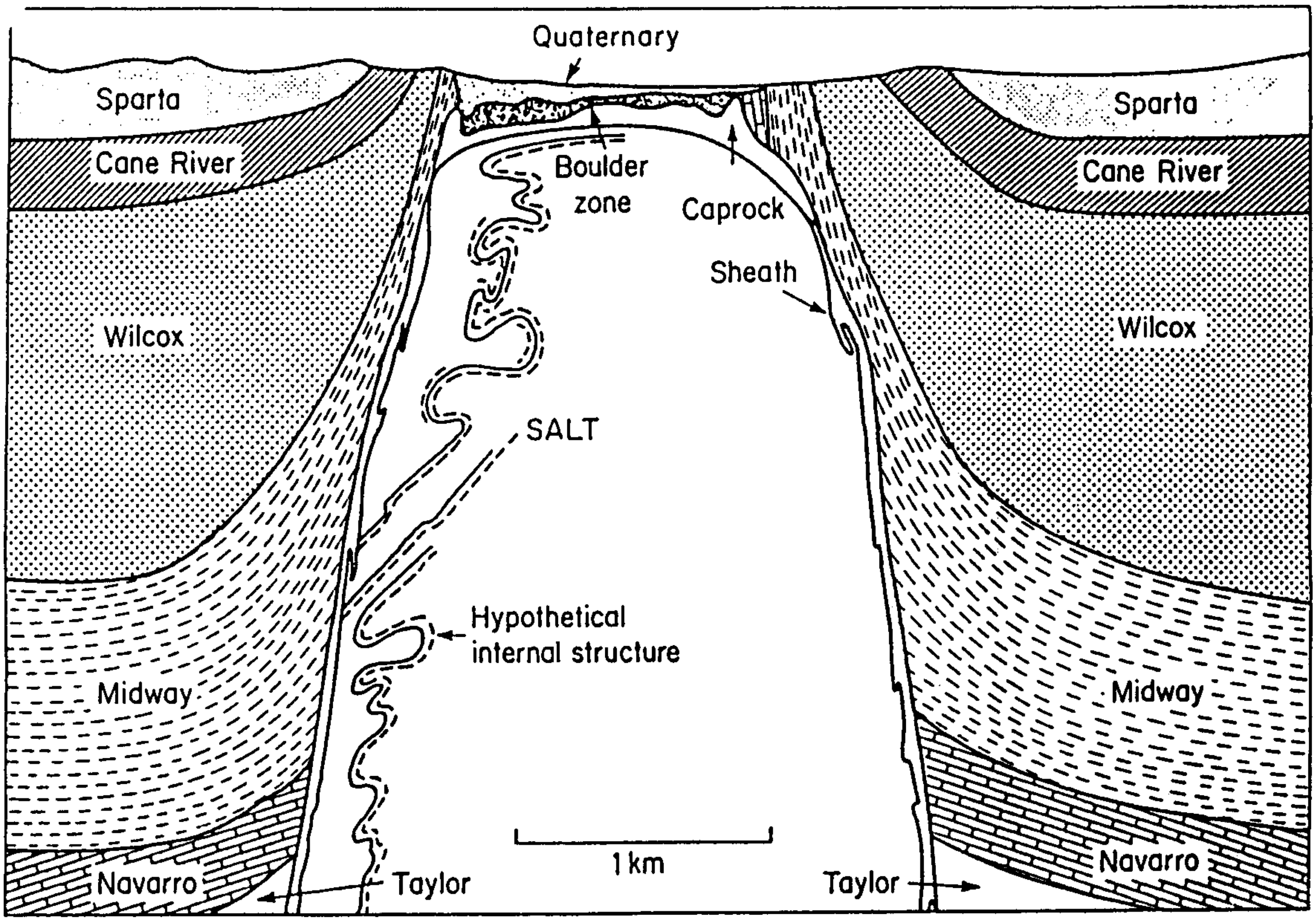

Figure 6.7 Cross-section of a typical salt dome (Rayburn's dome in Louisiana, USA), showing the contorted structure of originally horizontal evaporite beds within the dome, and the surrounding sediments upthrust during the rise of the dome. The presence of Quaternary sediments on the top of the dome indicates that it has been exposed at the

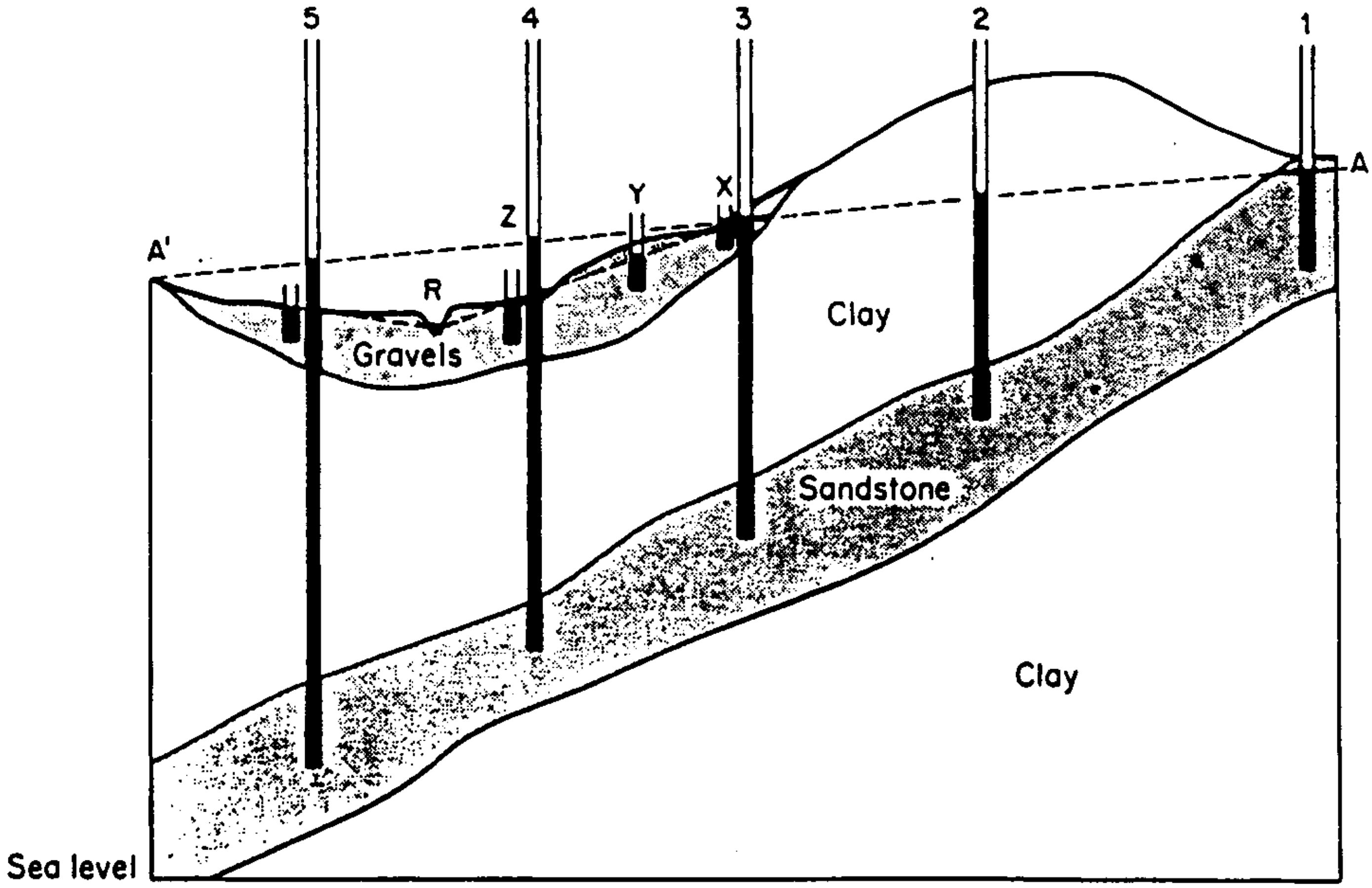

Figure 6.8 Simplified, and highly schematic illustration of hydraulic 'head'. If pipes were sunk into various points in the sandstone aquifer, then water would rise in them to the levels indicated in response to the head at each point. The hydraulic gradient, 'A–A'', controls the direction and rate of groundwater flow in the aquifer: water moves down gradient. Pipes 1–3 could represent ordinary water wells whereas 4–5 demonstrate what are often loosely referred to as 'artesian' conditions in a confined part of the aquifer. Wells at these points would overflow at the ground surface. The heads in the river (R) valley gravels (pipes X–Z) are close to the surface and in this case the line showing the hydraulic gradient in this aquifer unit also represents the water table, and the closely stippled area above it is the unsaturated zone. None of these wells overflows. To the left of pipe 3, the heads in the sandstone are higher than those in the gravels, and there is consequently a vertical hydraulic gradient which would allow very slow seepage of groundwater from the sandstone upwards through the intervening clay, into the gravels. If heads in the upper clay formation were higher than those in the aquifers, then seepage of clay groundwaters might occur both upwards and downwards into the gravels and sandstones. The importance of knowing the heads through such a series of formations in order to predict directions and rates of groundwater movement is clear. Head is usually measured in metres above sea-level

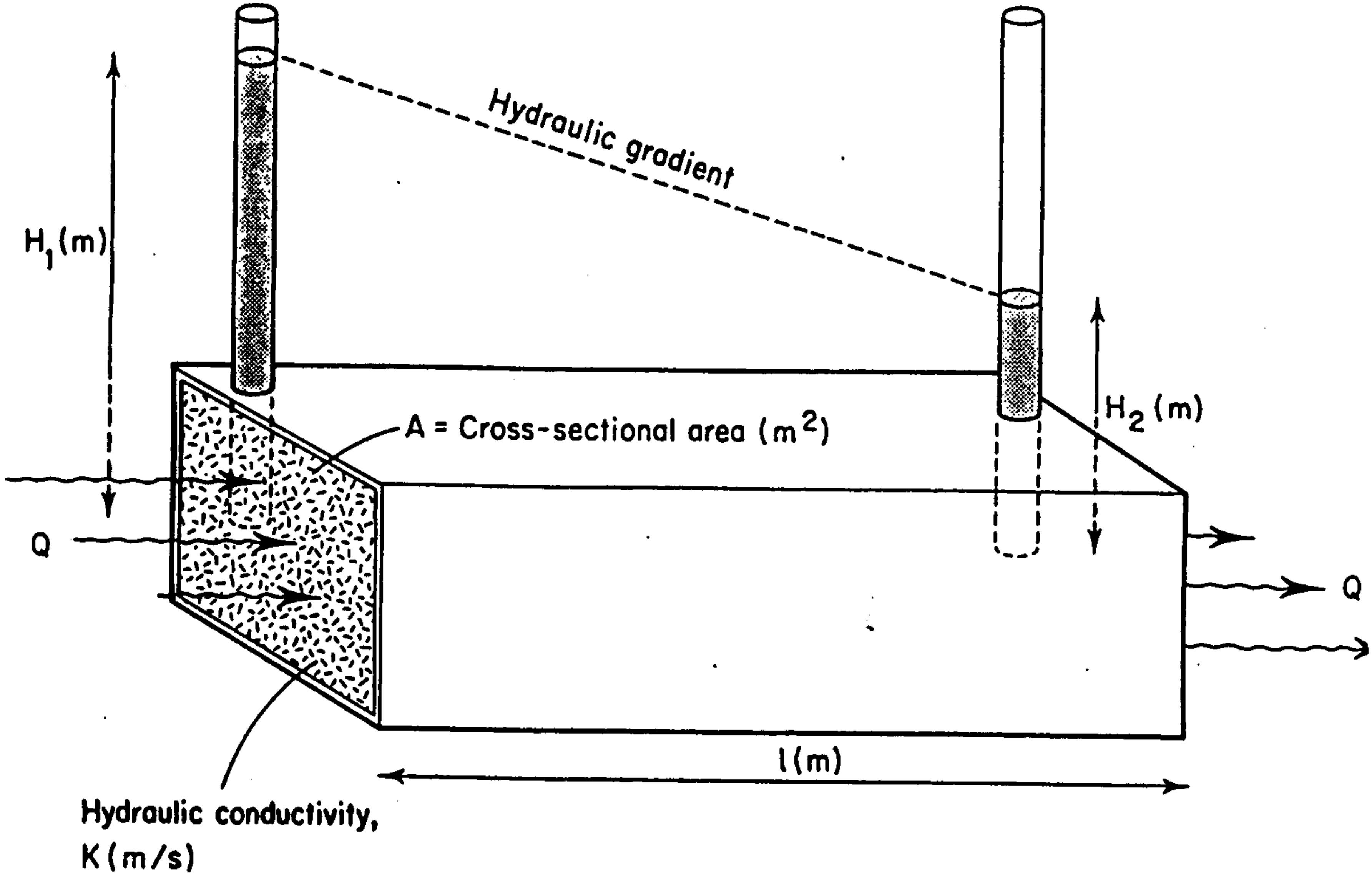

$$\text{Flux}(Q)\text{ in } m^3/s = K\underbrace{\left(\frac{H_1 - H_2}{l}\right)}_{\text{Hydraulic gradient (dimensionless)}}A$$

Figure 6.9 Schematic representation of D...

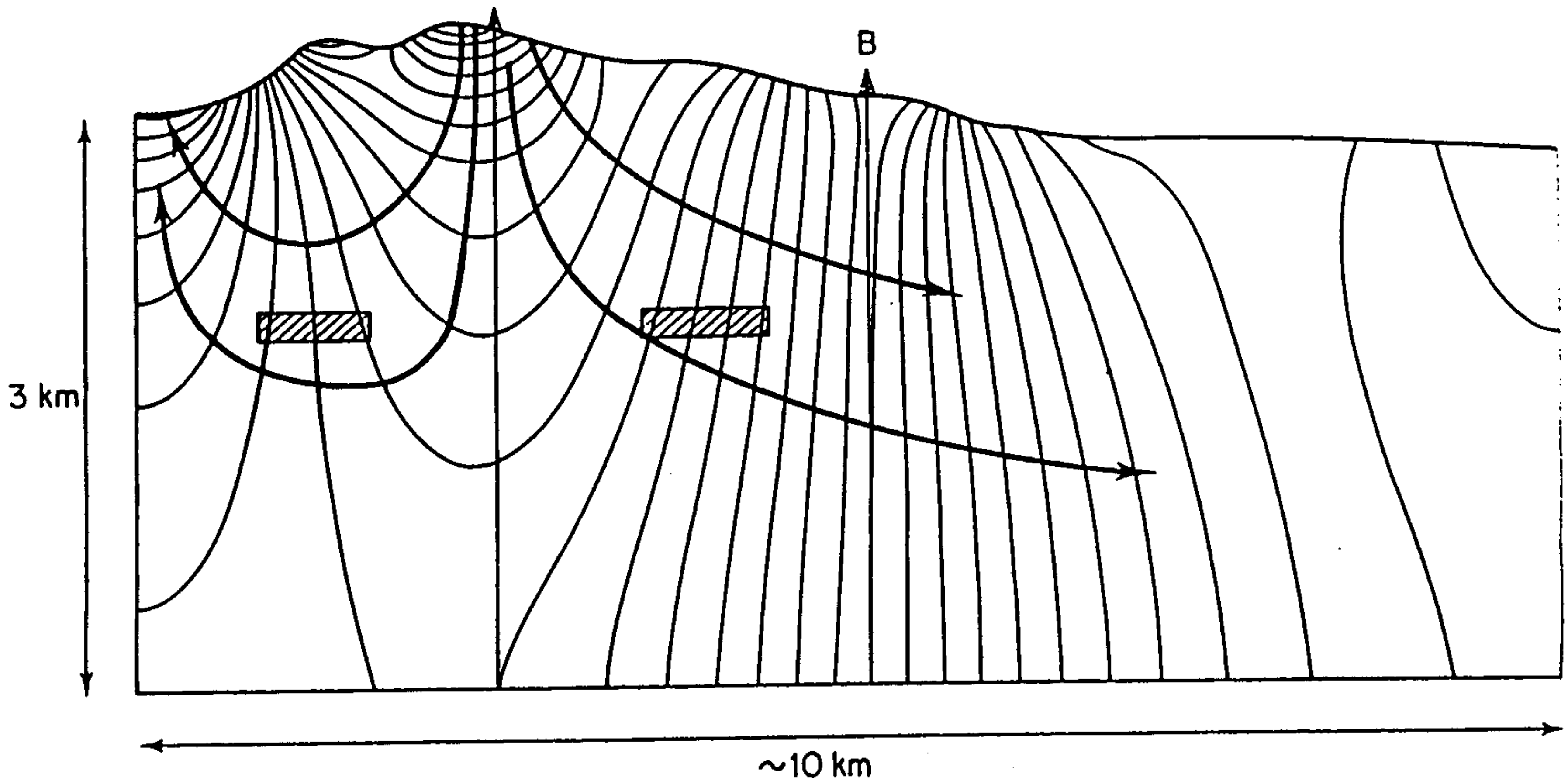

Figure 6.13 Typical results of a very simple two-dimensional finite element model of groundwater flow. A block of crystalline rock, with zero-flow boundaries assumed at the base and sides, and hydraulic conductivity decreasing progressively with depth. The curves are equipotentials (simply, lines of equal groundwater head), which can be seen to be controlled by the topography. Groundwater would flow down a potential gradient, that is at right angles to these equipotentials. A borehole at A would encounter progressively decreasing heads with depth, while one at B would find similar head values throughout the whole borehole. Some possible flow paths are shown. Flow volumes and velocities will decrease markedly with depth. The repository situated on the right appears to be in a better position than the one on the left, as pathlengths are potentially both

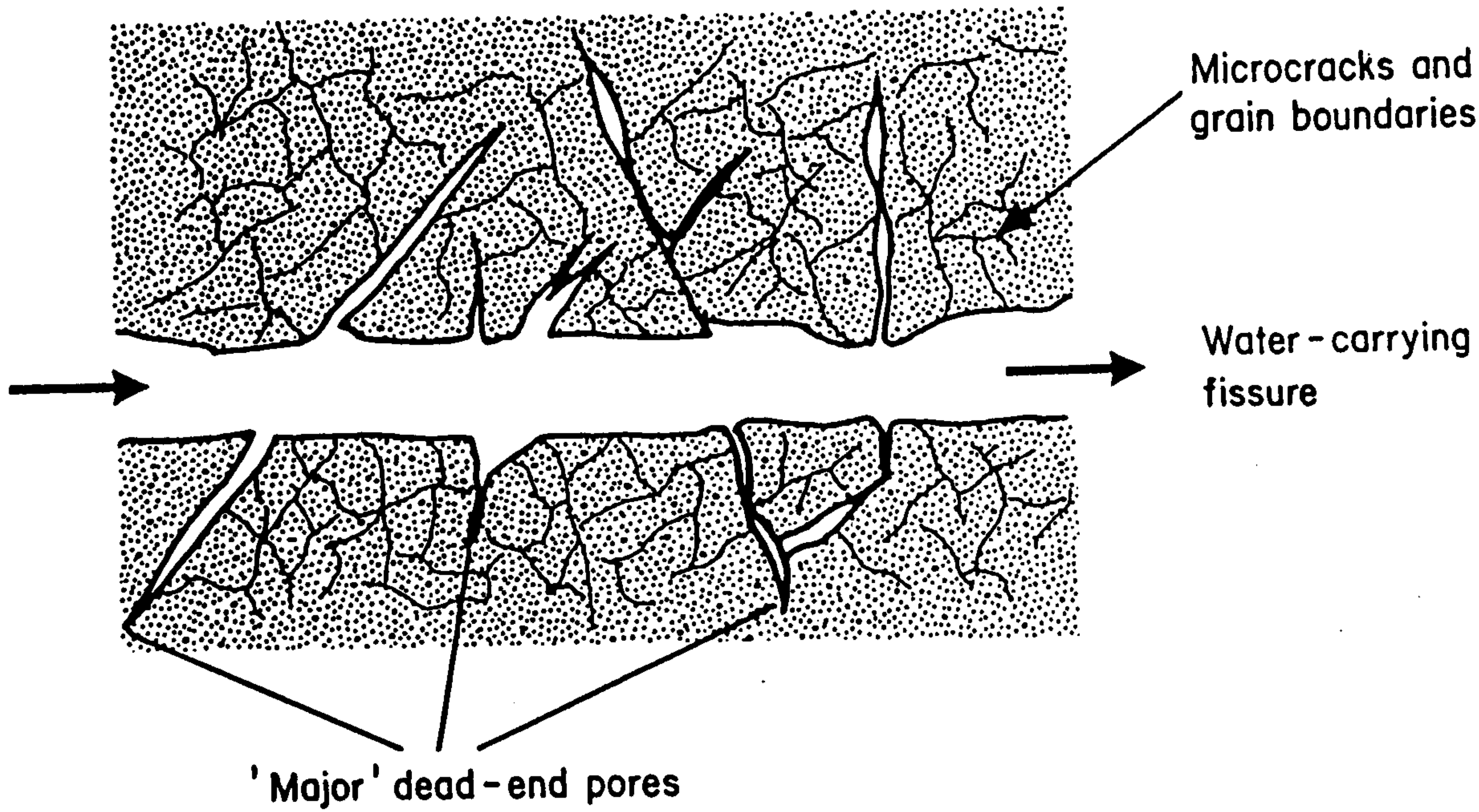

Figure 6.17 Microcracks and dead-end pores which may permit matrix diffusion in fractured rocks (see text)

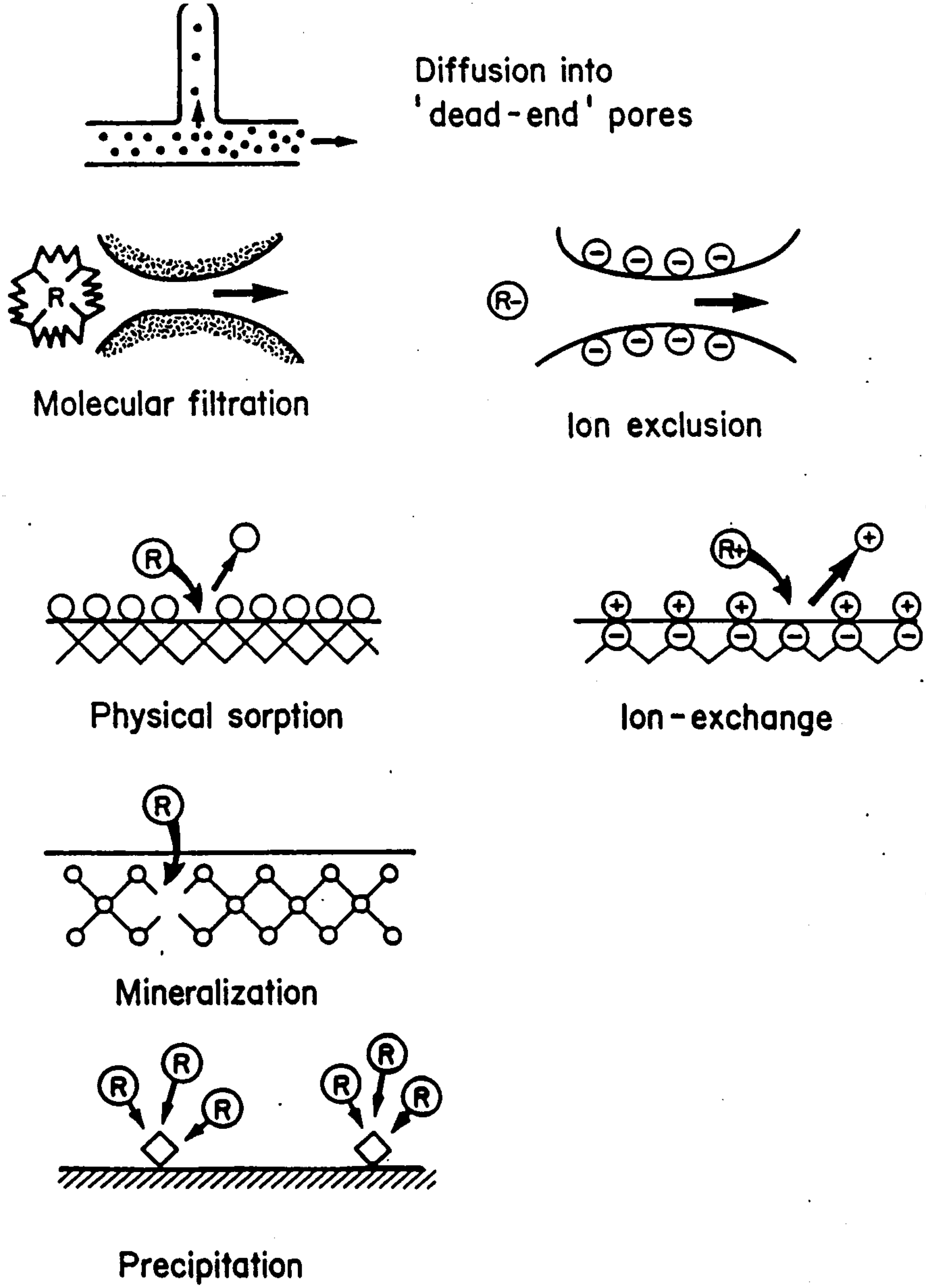

Figure 6.18 Schematic representation of the many possible retardation mechanisms possible as a result of interaction between

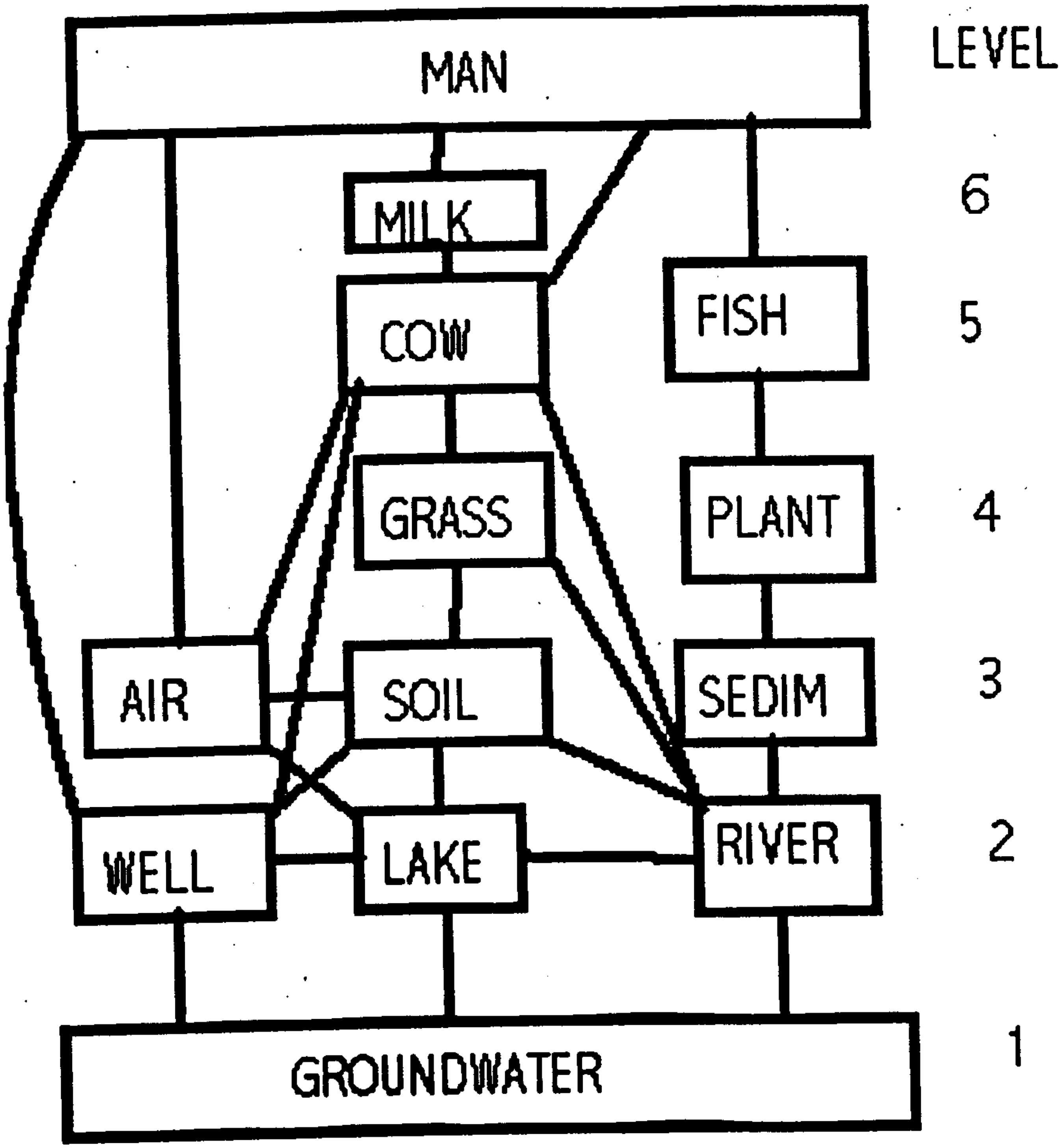

BIOSPHERE MODELLING

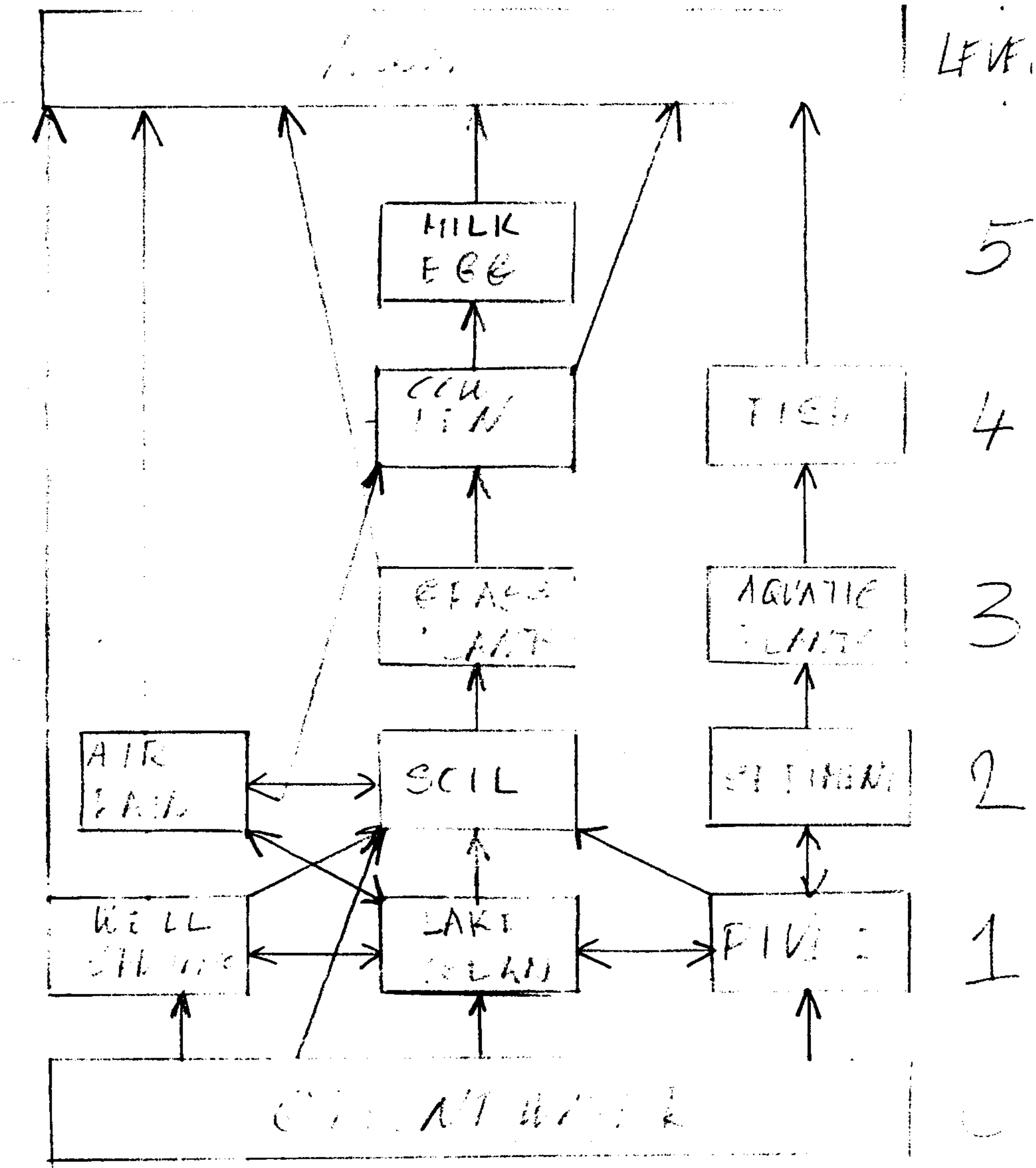

Fig

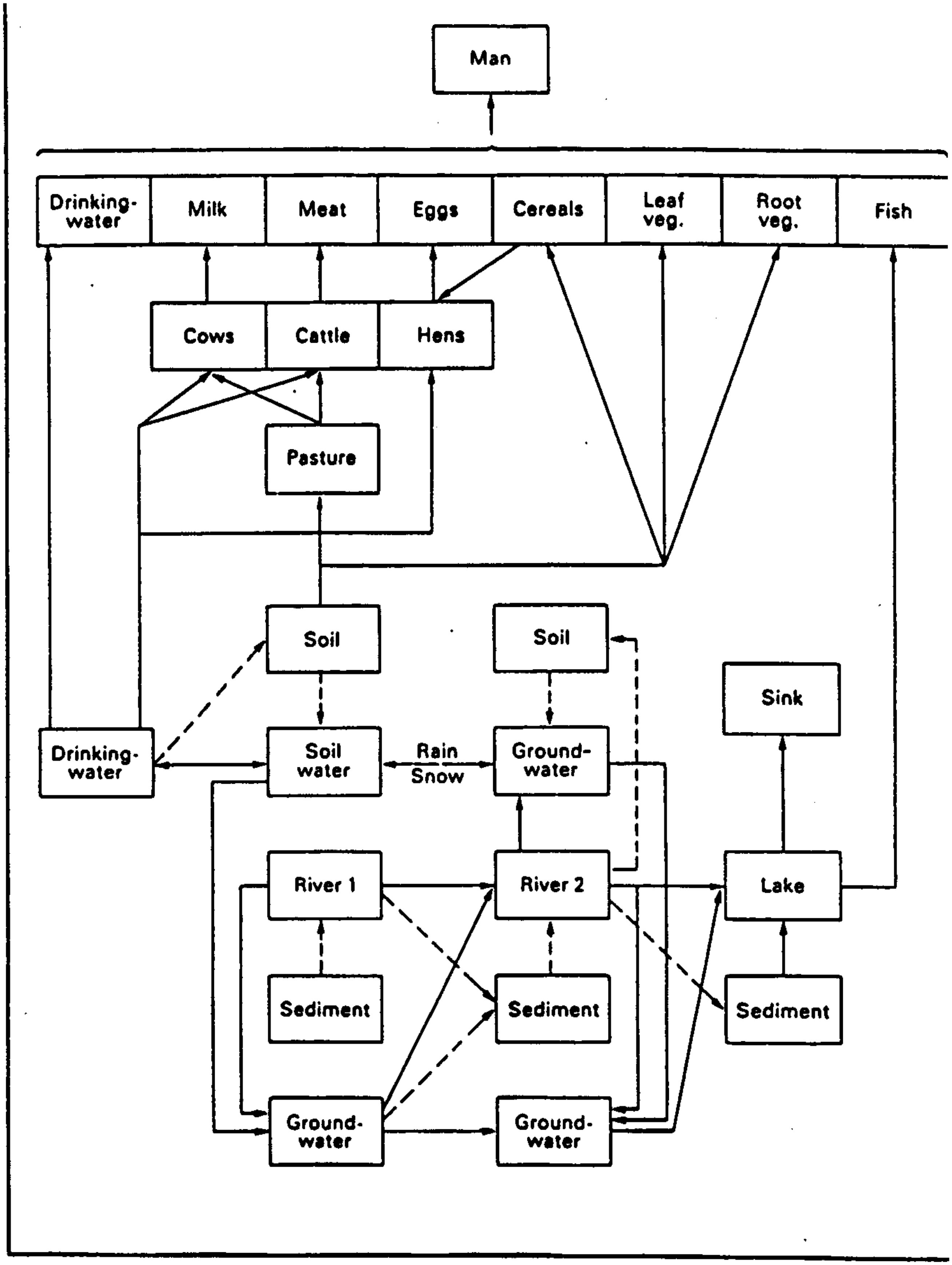

Figure 10.2 Typical compartments used in biosphere transport calculatio
(after Nagra, 1985). *Reproduced by permission of Nagra, Switzerland*

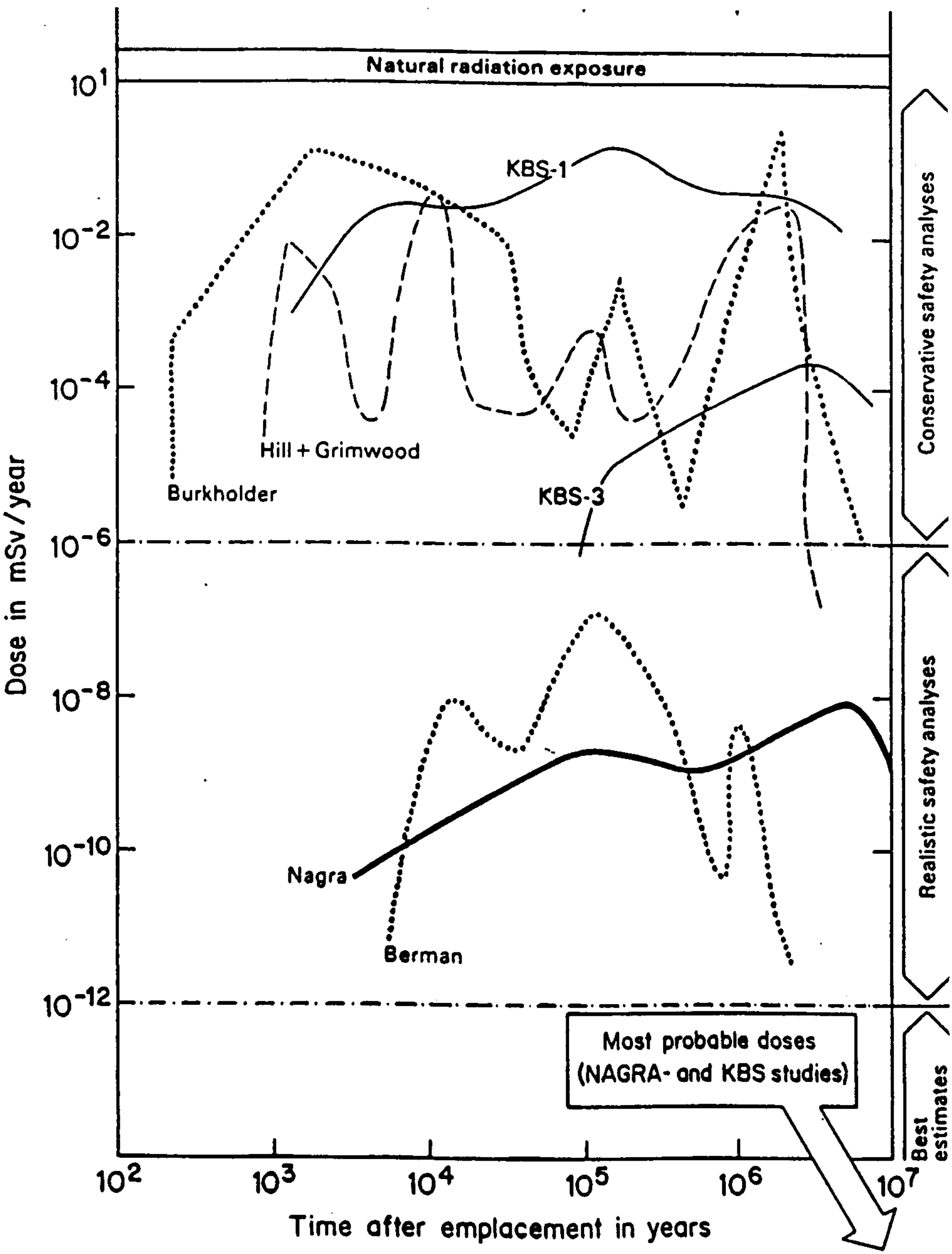

Figure 10.3 Radiation doses calculated in some important safety analyse

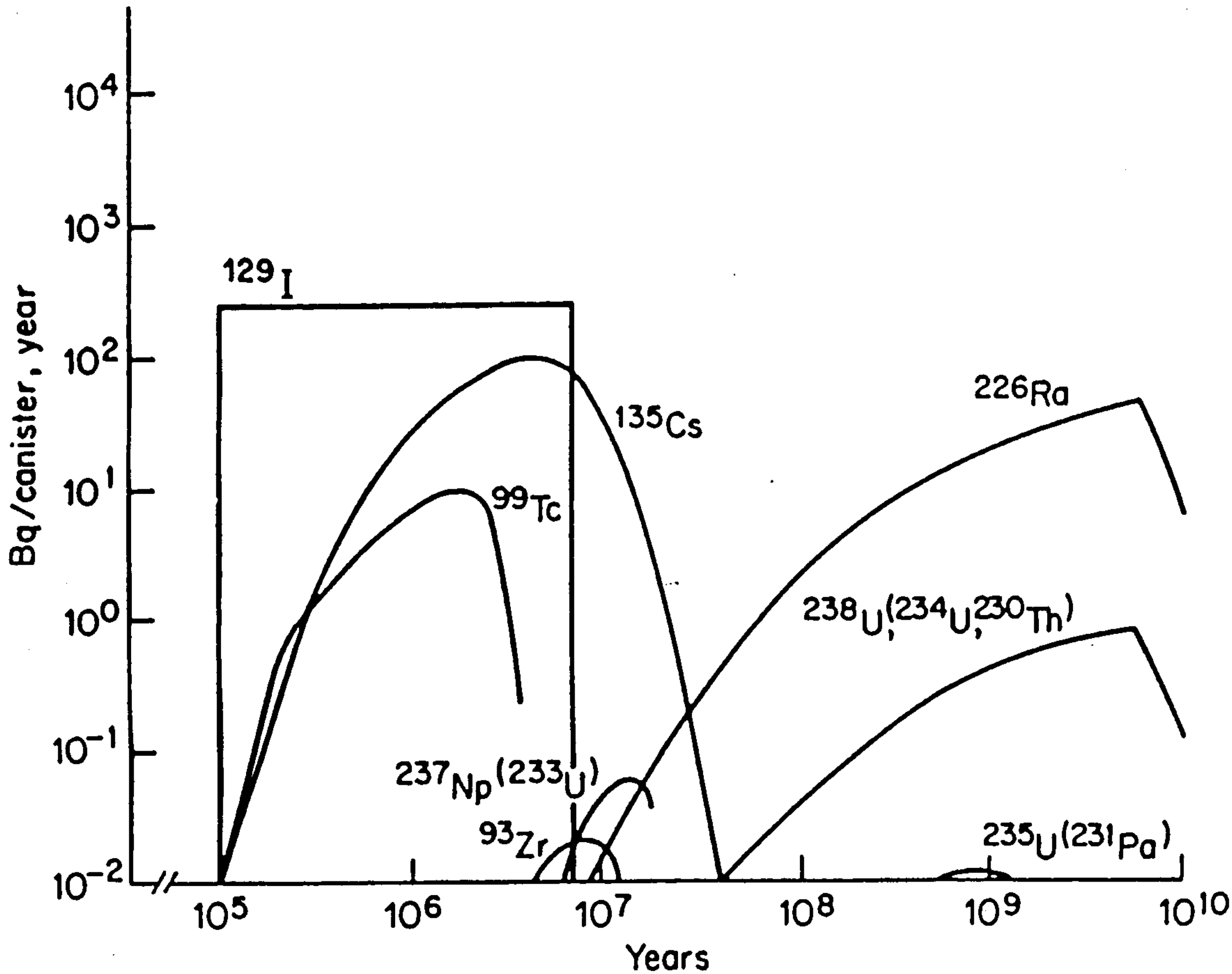

Figure 10.4 Results of the KBS-3 study. Releases to the biosphere (in Bq per container of waste per year) as a function of time after fuel discharge

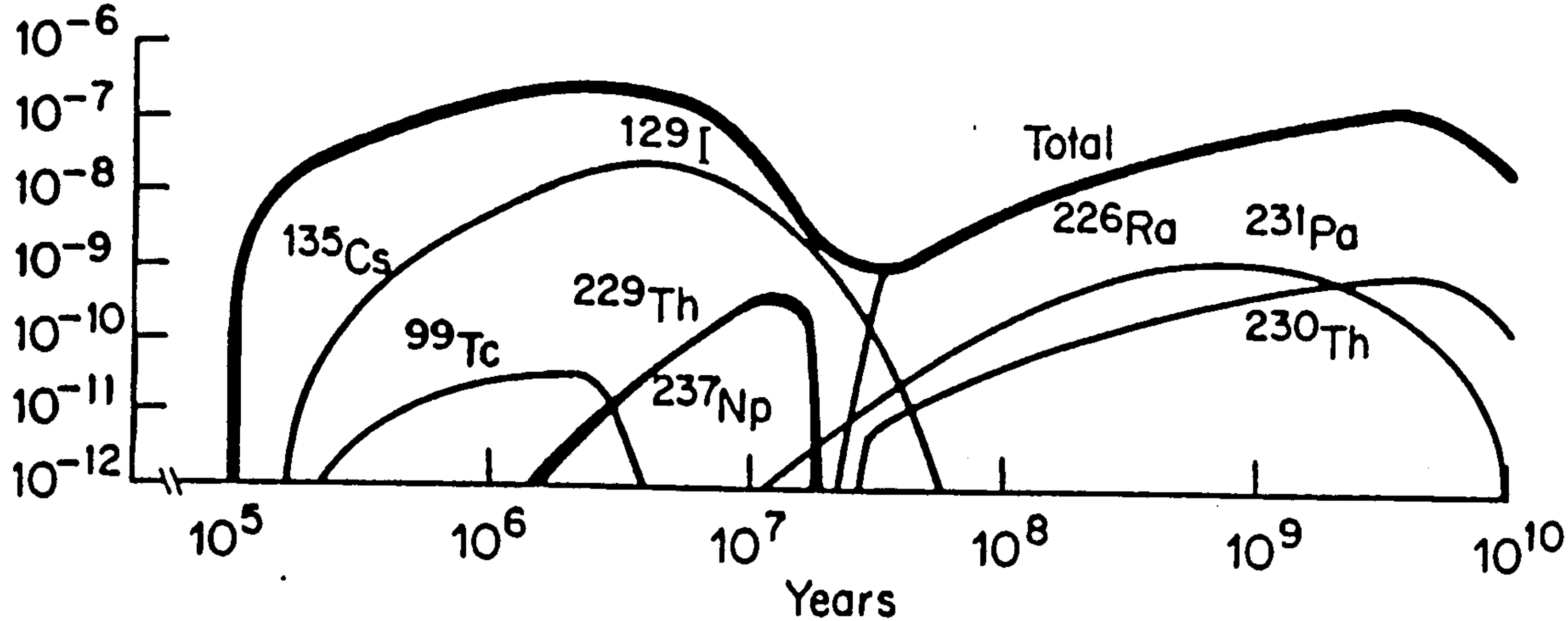

-igure 10.5 Calculated doses in the KBS-3 central scenario (see text)

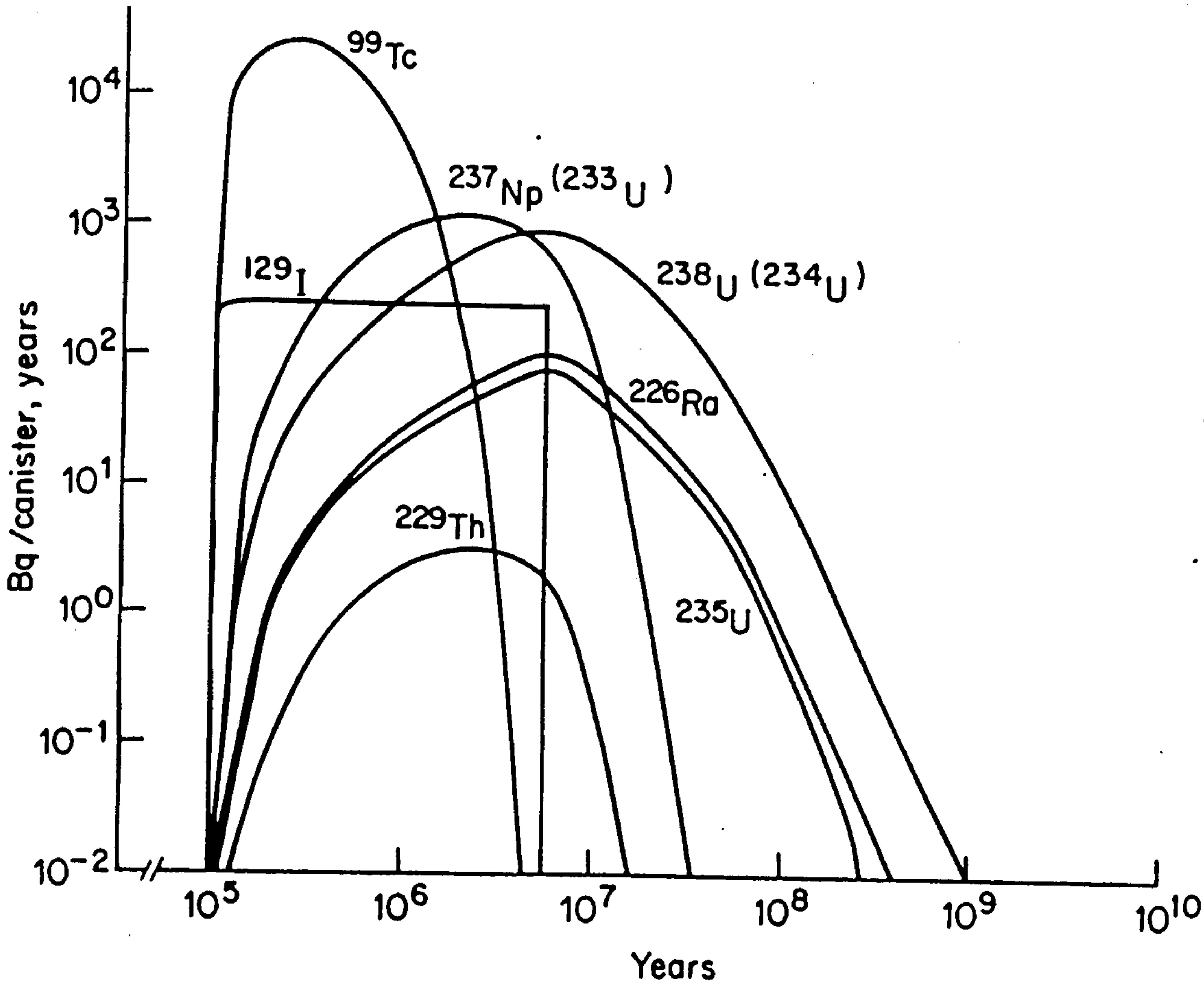

Figure 10.6 KBS-3 releases to the biosphere (Bq/container/year) for the

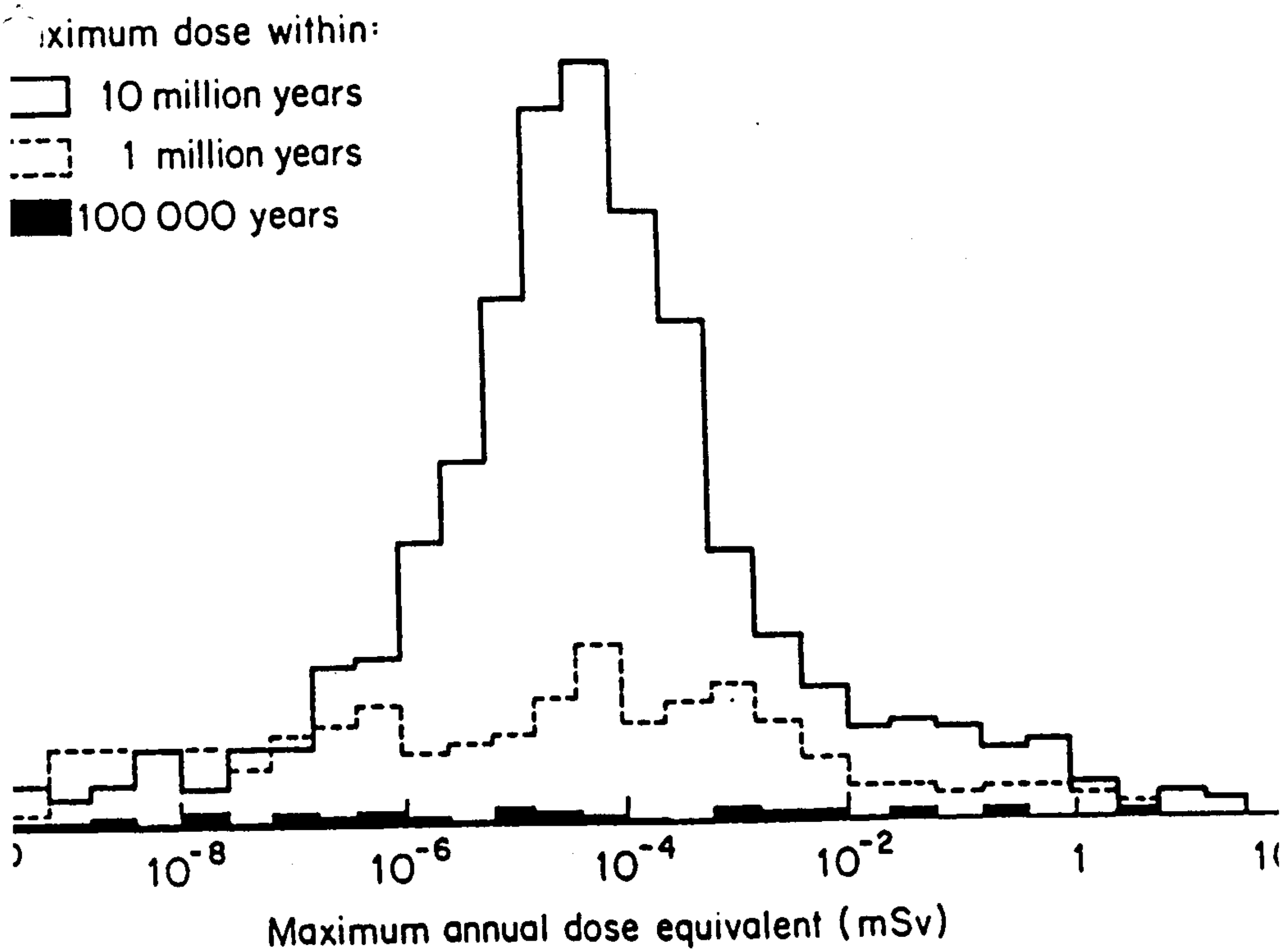

.0 Typical results of the Canadian SYVAC probabilistic sal
code, run for a HLW repository in crystalline basement rocks (fr
985). Maximum doses which result from each simulation are plot
of a histogram. A single simulation takes randomly selected val
;e for each parameter involved in the complete release and migrat
d in the code. The histogram thus shows the most proba
:e of the disposal system. It can be seen that for times up to 10^5 ye
simulations leads to doses greater than natural background (aro
at very long times into the future (10^7 years) the most probable do